Organic & Biomolecular Chemistry

PAPER

View Article Online
View Journal | View Issue

Cite this: *Org. Biomol. Chem.*, 2014, **12**, 1135

Synthesis of bicyclic organo-peptide hybrids *via* oxime/intein-mediated macrocyclization followed by disulfide bond formation†

Jessica M. Smith, Nicholas C. Hill, Peter J. Krasniak and Rudi Fasan*

Received 9th November 2013,
Accepted 18th December 2013

DOI: 10.1039/c3ob42222d

www.rsc.org/obc

A new strategy is described to generate bicyclic peptides that incorporate non-peptidic backbone elements starting from recombinant polypeptide precursors. These compounds are produced *via* a one-pot, two-step sequence, in which peptide macrocyclization by means of a bifunctional oxyamine/1,3-amino-thiol synthetic precursor is followed by intramolecular disulfide formation between the synthetic precursor-borne thiol and a cysteine embedded in the peptide sequence. This approach was found to be compatible with the cysteine residue occupying different positions within 8mer and 10mer target peptide sequences and across different synthetic precursor scaffolds, thereby enabling the formation of a variety of diverse bicyclic scaffolds.

Introduction

Macrocyclization constitutes an attractive approach for enhancing the conformational and binding properties of peptide-based molecules. Restriction of the conformational flexibility of these compounds by means of various ring-forming strategies[1] often results in improved proteolytic resistance[2–4] and more favourable membrane crossing properties,[5–7] in addition to enhanced binding affinity and selectivity toward a target protein.[8–14] Furthermore, macrocyclic peptide-based scaffolds have received increasing attention owing to their inherent ability to interact with extended and relatively shallow binding sites in biomolecules, and thus for their potential to address notoriously challenging targets such as misregulated protein–protein and protein–nucleic acid interactions involved in disease.[15–18]

In light of these advantageous features, a variety of strategies have been recently investigated to generate macrocyclic peptides starting from genetically encoded precursor polypeptides.[19,20] These approaches have involved the formation of cyclic peptides *via* split intein-catalyzed circular ligation,[21,22] chemical cross-linking with amine-[23] or cysteine-reactive reagents,[24,25] cyclization of *in vitro* translated peptides containing unnatural amino acids,[26,27] or manipulation of biosynthetic machineries involved in the biosynthesis of naturally occurring cyclopeptides.[28–34] Contributions from our group to this field have involved the development of methods for the generation of macrocyclic organic-peptide hybrids, referred to as "MOrPHs", through the chemoselective cyclization of ribosomally derived polypeptides *via* synthetic reagents.[35–37] In this system, a genetically encoded 'target peptide sequence' is flanked by an unnatural amino acid and an intein protein (*i.e.* GyrA intein), to furnish two orthogonally reactive functionalities at the N-terminal and C-terminal ends, respectively, of the peptide sequence. Cyclization of these precursor polypeptides is then achieved upon reaction with a bifunctional synthetic precursor (SP) to form a side-chain-to-C-end macrocyclic product. In a recently reported catalyst-free variation of this strategy[37] (Scheme 1), oxyamine/1,3-amino-thiol synthetic precursors proved effective in promoting efficient MOrPH formation *via* (i) a transesterification/S-to-N acyl shift reaction mediated by the SP amino-thiol moiety at the level of the C-terminal thioester group of the target peptide ('a' → 'b', Scheme 1), (ii) followed by ring closure upon reaction of the SP-borne oxyamino functionality with the side-chain keto group provided by the unnatural amino acid *para*-acetylphenylalanine ('b' → 'c', Scheme 1). This macrocyclization strategy was found to be compatible with significant variations in both the length (4mer to 15mer) and composition of the target peptide sequence and the nature of the synthetic precursor.[37]

Beyond macrocyclization, further rigidification of a peptidic backbone can be achieved through installation of additional intramolecular cross-links. Notably, bi- and polycyclic topologies are exhibited by a number of cyclopeptide natural products that exhibit a variety of interesting bioactivities from

Department of Chemistry, University of Rochester, Rochester, NY 14627, USA. E-mail: fasan@chem.rochester.edu

†Electronic supplementary information (ESI) available: Oligonucleotide sequences, additional MS spectra and chemical structures of bicyclic products. See DOI: 10.1039/c3ob42222d

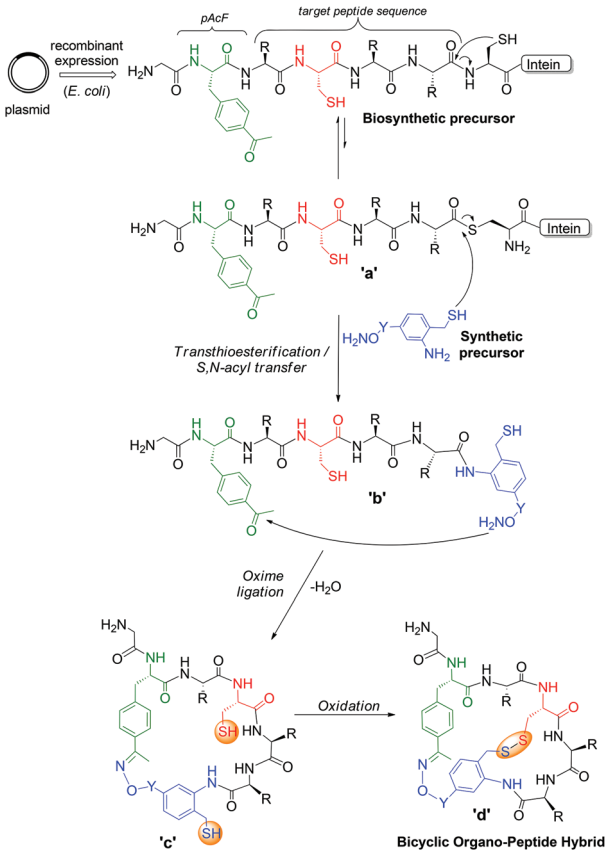

Scheme 1 Strategy for synthesis of bicyclic organo-peptide hybrids (BOrPHs) *via* chemoselective cyclization of intein-fusion precursor polypeptides followed by oxidative disulfide bond formation. The oxyamine/1,3-amino-thiol synthetic precursor, the unnatural amino acid (*p*-acetyl-Phe), and the reactive cysteine residue within the target peptide sequence are highlighted in blue, green, and red, respectively.

cytotoxic to antimicrobial activity (*e.g.* defensins, cyclotides, lanthipeptides).[38–40] Over the past decade, a number of notable strategies have been reported for the chemical synthesis of peptides in bicyclic arrangements.[41–46] In contrast, much fewer methods are currently available for the bicyclization of ribosomally derived peptides.[47–49] In this report, we describe the development and investigation of a novel, versatile strategy to access ribosomally-derived bicyclic organo-peptide hybrids (BOrPHs) which are constrained by virtue of a side-chain-to-C-end cyclic backbone combined with an intramolecular disulfide bond.

Results and discussion

Design of bicyclization strategy

As described in Scheme 1, MOrPHs formed by means of oxyamino/1,3-amino-thiol synthetic precursors (SPs) feature a free thiol functionality as a result of the S-to-N acyl transfer rearrangement occurring after SP-mediated attack at the level of the thioester group at the junction between the target peptide sequence and the intein. In the course of previous studies, we established that this rearrangement proceeds rapidly and quantitatively regardless of the length of the peptide target sequence and of the nature of the amino acid residue preceding the intein,[37] presumably as a result of the readily accessible six-membered transition state involved in the intramolecular acyl transfer process. Based on this information, we reasoned that the SP-borne thiol functionality embedded into the organo-peptide macrocycle product obtained after cyclization could be exploited to form an intramolecular disulfide bridge with a cysteine residue located within the peptidic portion of the macrocycle (Scheme 1, 'c' → 'd'). If viable, we envisioned this strategy could provide a convenient route to access different bicyclic topologies by simply varying the position of the cysteine residue within the target peptide sequence.

Reactivity and macrocyclization of 8mer cysteine-containing precursor polypeptides

To test this idea, we initially generated a series of protein constructs of the type MG-(pAcF)-X_8-GyrA, in which a cysteine residue was introduced at each non-terminal position of the eight amino acid-long target peptide sequence (Table 1), *i.e.* from position U + 1 (U = unnatural amino acid, pAcF) to position U + 7. These protein constructs were produced in *E. coli* cells co-transformed with a pET22- and a pEVOL-based vector for the expression, respectively, of the corresponding precursor protein and of an engineered *Mj*$tRNA_{CUA}$/*Mj*-tyrosyl-tRNA synthetase (*Mj*TyrRS) pair for the incorporation of the pAcF *via* amber stop codon suppression.[50] The proteins were expressed in minimal media supplemented with pAcF and purified *via* nickel-affinity chromatography using a poly-histidine tag fused to the C-terminus of the GyrA intein. The identity of the purified proteins was then confirmed by SDS-PAGE and MALDI-TOF mass spectrometry.

To induce macrocyclization, the triazole-based synthetic precursor **1** (SP6, Fig. 1) was first tested as this reagent was

Table 1 Amino acid sequences of the precursor polypeptides investigated in this study. The unnatural amino acid *p*-acetyl-Phe (pAcF) and cysteine residue are highlighted in green and red, respectively

Construct	Biosynthetic precursor
MG8_U + 1	MGpAcFCGSAEYGT-GyrA
MG8_U + 2	MGpAcFTCSAEYGT-GyrA
MG8_U + 3	MGpAcFTGCAEYGT-GyrA
MG8_U + 4	MGpAcFTGSCEYGT-GyrA
MG8_U + 5	MGpAcFTGSACYGT-GyrA
MG8_U + 6	MGpAcFTGSAECGT-GyrA
MG8_U + 7	MGpAcFTGSAEYCT-GyrA
MG10_U + 1	MGpAcFCGSKLAEYGT-GyrA
MG10_U + 2	MGpAcFTCSKLAEYGT-GyrA
MG10_U + 3	MGpAcFTGCKLAEYGT-GyrA
MG10_U + 4	MGpAcFTGSCLAEYGT-GyrA
MG10_U + 5	MGpAcFTGSKCAEYGT-GyrA
MG10_U + 6	MGpAcFTGSKLCEYGT-GyrA
MG10_U + 7	MGpAcFTGSKLACYGT-GyrA
MG10_U + 8	MGpAcFTGSKLAECGT-GyrA
MG10_U + 9	MGpAcFTGSKLAEYCT-GyrA

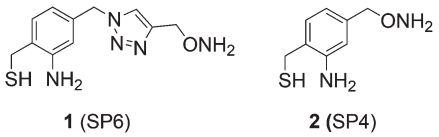

Fig. 1 Chemical structures of the oxyamine/amino-thiol synthetic precursors used in this study.

previously found to afford the desired MOrPHs in high yields.[37] For these reactions, the intein-fusion proteins (100 μM) were incubated with **1** (10 mM) in phosphate buffer (pH 7.5) supplemented with TCEP (10 mM) as a thiol reducing agent. Under these conditions, nearly quantitative splicing of the intein-fusion proteins was observed after 5–6 hours as determined by LC-MS. To examine product formation, the reactions were then analyzed by MALDI-TOF mass spectrometry. The protein constructs containing the cysteine residue at position U + 5, U + 6, U + 7 all afforded the desired macrocycle with no side products (Fig. 2A and S1 in ESI†), a result in line with those previously obtained in the context of target peptide sequences of similar length.[37] In contrast, the reactions of **1** with the protein constructs carrying a cysteine at positions U + 1, U + 2, U + 3, and U + 4 resulted in the formation of the desired **1**-containing MOrPH together with a second product of smaller molecular weight, as illustrated by the representative data corresponding to the MG8_U + 3 construct in Fig. 2B (see also Fig. S1 in ESI†).

The mass of this lower molecular weight species was found to be consistent with that of a thiolactone product produced by the intramolecular attack of the cysteine side-chain sulfhydryl group onto the intein thioester ("self-cyclized product" or "sc" in Scheme 2). To further verify the nature of this compound, the post-cyclization reaction mixtures were added with the thiol-alkylating reagent iodoacetamide. As expected, the MALDI-TOF MS signal corresponding to the MOrPH product disappeared to give rise to a +114 Da adduct, which is

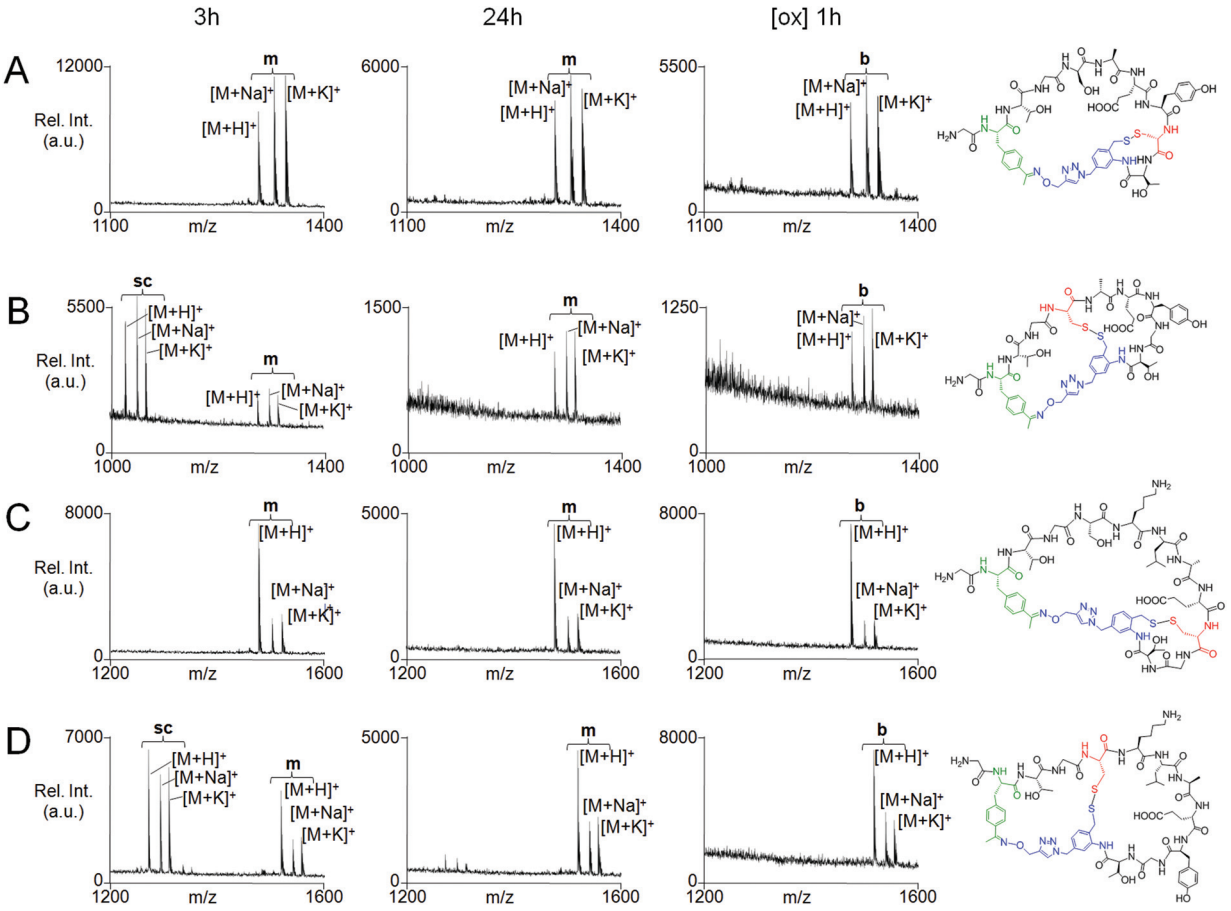

Fig. 2 MALDI-TOF MS analysis of the reactions between synthetic precursor **1** (SP6) and representative 8mer and 10mer precursor polypeptides: (A) MG8_U + 7; (B) MG8_U + 3; (C) MG10_U + 8; (D) MG10_U + 3. Spectra correspond to the three hour (*left*) and 24 hour time point (*center*) after addition of **1** and one hour time point after addition of BPDS (*right*). Peaks corresponding to the proton ($[M + H]^+$), sodium ($[M + Na]^+$), and potassium ($[M + K]^+$) adducts of the MOrPH ('m'), self-cyclized thiolactone ('sc') and bicyclic product ('b') are labeled. Chemical structures of the corresponding bicyclic products are also shown. (A) **MG8_U + 7**, '**m**': $[M + H]^+_{calc}$ 1307.5, $[M + H]^+_{obs}$ 1306.8, '**b**': $[M + H]^+_{calc}$ 1305.5, $[M + H]^+_{obs}$ 1304.8; (B) **MG8_U + 3**, '**m**': $[M + H]^+_{calc}$ 1277.5, $[M + Na]^+_{obs}$ 1276.7, '**sc**': $[M + H]^+_{calc}$ 1030.2, $[M + H]^+_{obs}$ 1029.6, '**b**': $[M + H]^+_{calc}$ 1275.5, $[M + H]^+_{obs}$ 1274.7; (C) **MG10_U + 8**, '**m**': $[M + H]^+_{calc}$ 1442.7, $[M + H]^+_{obs}$ 1442.1, '**b**': $[M + H]^+_{calc}$ 1440.7, $[M + H]^+_{obs}$ 1440.1; (D) **MG10_U + 3**, '**m**': $[M + H]^+_{calc}$ 1518.7, $[M + H]^+_{obs}$ 1517.9, '**sc** : $[M + H]^+_{calc}$ 1271.4, $[M + H]^+_{obs}$ 1270.8, '**b**': $[M + H]^+_{calc}$ 1516.7, $[M + H]^+_{obs}$ 1515.9.

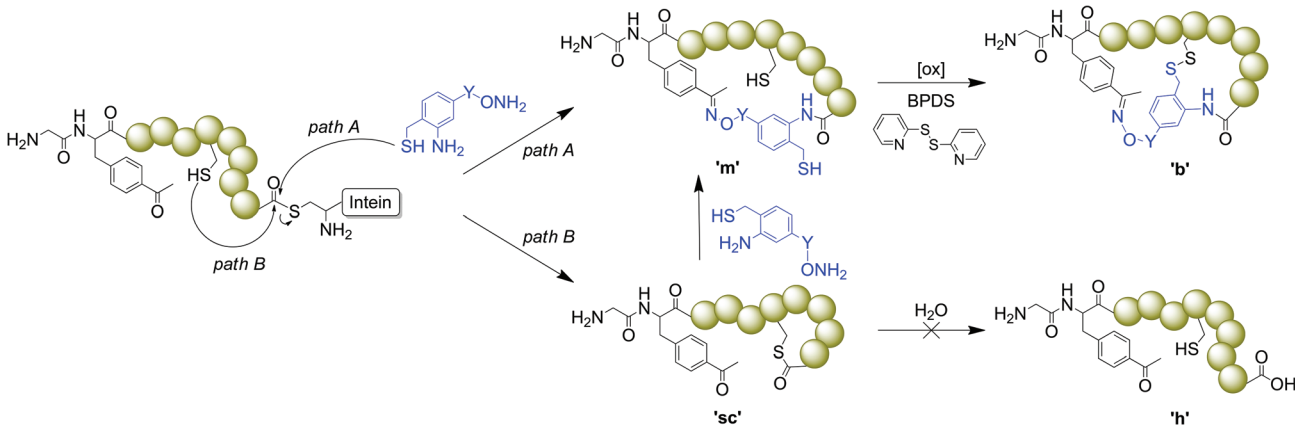

Scheme 2 Schematic representation of the reactions involved in the macro- and bicyclization of the cysteine-containing biosynthetic precursors with the oxyamine/1,3-amino-thiol synthetic precursors. The MOrPH and thiolactone intermediates and the final bicyclic product are labeled as 'm', 'sc', and 'b', respectively.

consistent with the macrocycle product being alkylated at the level of both the sulfhydryl group of the SP moiety and the internal cysteine residue (Fig. S5 in ESI†). In contrast, the mass of the self-cyclized product remained unchanged after exposure to iodoacetamide (Fig. S5 in ESI†), indicating the presence of no free thiol groups in this compound and thus further confirming its assignment to the thiolactone structure.

Another interesting observation concerned the fact that while formation of the thiolactone species was found to predominate at short reaction times (3 hours), a progressive increase in the MOrPH-to-thiolactone ratio generally occurred at longer incubation times. Indeed, for the constructs with the cysteine at position U + 2 and U + 4, the relative amount of the MOrPH product increased from about 15–20% at the 3 hour time point to 60–70% after 24 hours, as estimated based on the relative intensity of the corresponding peaks in the MALDI-TOF spectra and assuming the two species share similar ionization properties (Fig. S1 in ESI†). For the MG8_U + 1 and MG8_U + 3 constructs, complete conversion of the thiolactone species to the desired MOrPH product was achieved after 24 hours incubation with **1** (Fig. 2B and S1 in ESI†). The same result was obtained for the aforementioned MG8_U + 2 and MG8_U + 4 constructs after more extended incubation times (*i.e.* 36 h). These trends likely reflect the differential stability of the thiolactone product formed in each case.

Altogether, these results pointed at the occurrence of two types of reactivity for the series of 8mer cysteine-containing precursor polypeptides of Table 1. Specifically, for the constructs where the cysteine is most proximal to the intein thioester (*i.e.* separated from the thioester linkage by one (MG8_U + 7) to three amino acid residues (MG8_U + 5)), intramolecular transthioesterification does not effectively compete with SP-induced macrocyclization. In contrast, for the constructs where the cysteine residue is located at longer distances from the intein thioester (*i.e.* 5 to 8 amino acid residues apart), thiolactonization appears to be kinetically favored over MOrPH formation (Scheme 2). The differential reactivity of these constructs can be rationalized on the basis of the larger strain associated with the smaller size thiolactone rings (*i.e.* 13 to 7 membered rings) which would be formed from the constructs MG8_U + 5 to MG8_U + 7 as compared to the other protein constructs of the series (*i.e.* 16 to 24 membered rings).[51] The higher propensity of the latter to undergo cysteine-mediated self-cyclization is also consistent with the larger extent of premature splicing observed for these proteins (30–40%) during recombinant expression in *E. coli* as compared to the U + 5, U + 6, and U + 7 constructs (<5%). Despite this somewhat unexpected reactivity, our data also clearly indicate that the thiolactone by-product can be intercepted by the synthetic precursor and further converted into the thermodynamically more stable MOrPH product over time, as schematically summarized in Scheme 2. This outcome is likely driven by the irreversible S-to-N acyl transfer at the level of the *ortho*-amino-methylmercaptan-aryl moiety of the synthetic precursor. Furthermore, the observation of no linear by-products (*i.e.* product 'h' in Scheme 2) indicates that SP insertion into the thiolactone ring effectively outcompetes hydrolysis of the latter, resulting in the observed accumulation of the MOrPH product over time.

Generation of 8mer-based bicyclic organo-peptide hybrids

Having established the formation of the desired MOrPHs for all the 8mer precursor peptide sequences, we then focused on exploring the possibility to further convert these products into bicyclic organo-peptide hybrids *via* thiol oxidation according to the general strategy outlined in Scheme 1. Our initial attempts to promote the formation of the desired intramolecular disulfide bridge *via* oxidation with air or iodine (I_2) resulted in the formation of only trace amounts of the target bicyclic product, even after prolonged reaction times (>20 hours). As an alternative method, the oxidation step was carried out using the reagent 2,2'-bis-pyridyldisulfide (BPDS), which was previously reported to favour disulfide formation in synthetic peptides.[52] Gratifyingly, we found that in the presence of BPDS

(10 mM), all of the seven 8mer-based MOrPHs could be efficiently converted to the desired bicyclic organo-peptide hybrids within a short time (1 hour), as indicated by the disappearance of the signal corresponding to the MOrPH species and appearance of a signal at −2 *m*/*z* units in the MALDI-TOF MS spectra (Fig. 2A–B and S1†). Formation of the intramolecular disulfide linkage was further probed by treatment of the post-oxidation products with iodoacetamide. Under these conditions, no alkylation was observed for any of the seven constructs tested, which confirmed the absence of free thiols in these compounds and indicated that disulfide formation proceeded quantitatively. The bicyclic products were analyzed by LC-MS and MS/MS to further validate their structure. Consistent with the MALDI-TOF MS data, LC-MS analysis displayed a −2 Da mass difference for the macrocyclic compound before and after oxidation (Fig. 3A). The structural difference between the monocyclic and corresponding bicyclic product was further evidenced by the difference in elution times (Fig. 3A).

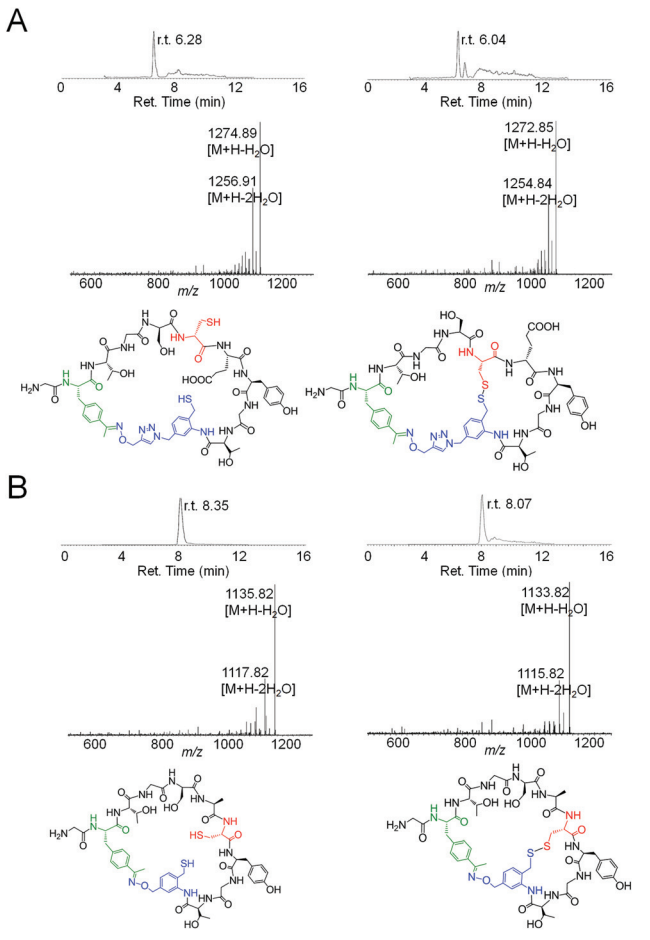

Fig. 3 LC-MS and MS/MS analysis of the macrocyclic ('m') and bicyclic ('b') products obtained from the reactions of (A) synthetic precursor **1** and precursor protein MG8_U + 4; and (B) synthetic precursor **2** and precursor protein MG8_U + 5. *Left panel*: extracted ion chromatogram (*top*), MS/MS spectrum (*middle*), and chemical structure of the MOrPH product (*bottom*). *Right panel*: extracted ion chromatogram (*top*), MS/MS spectrum (*middle*), and chemical structure of the corresponding post-oxidation bicyclic product (*bottom*).

Finally, the MS/MS spectra of these compounds indicated a backbone fragmentation pattern consistent with that of a cyclic peptide. Taken together, these data demonstrated that all the cysteine-containing 8mer/**1**-based MOrPHs could be rapidly and quantitatively converted into their bicyclic counterparts *via* a simple, single-pot procedure. Notably, bicyclization could be achieved by engaging a cysteine residue located at any of the non-terminal positions of the 8mer target peptide sequence, providing access to an array of diverse bicyclic topologies (Fig. 2A–B and S1 in ESI†).

Reactivity and bicyclization of 10mer target peptide sequences

Encouraged by these results, we wished to test the feasibility of this bicyclization strategy across a peptide target sequence of different (*i.e.* longer) length. To this end, we constructed and expressed a series of biosynthetic precursors containing a 10mer peptide target sequence of the type MG-(pAcF)-$(X)_{10}$-GyrA (Table 1). As for the 8mer constructs, a cysteine was placed at each of the non-terminal positions of the model peptide sequence, *i.e.* from position U + 1 through U + 9. Macrocyclization reactions were carried out by incubating the nine protein constructs with compound **1** as described above. MS analyses proved that all reactions resulted in the complete consumption of the full-length precursor protein as evidenced by the disappearance of the corresponding peak in LC-MS spectra. Interestingly, the 10mer constructs were found to exhibit similar reactivity trends as observed for the 8mer constructs. Indeed, **1**-induced macrocyclization was completely favored over cysteine-mediated self-cyclization for the constructs in which the cysteine residue was within four residues from the intein-catalyzed thioester linkage (MG10_U + 7, MG10_U + 8, MG10_U + 9), as illustrated by the representative MS spectra in Fig. 2C (see also Fig. S2†). For the remaining constructs (MG10_U + 1 through MG10_U + 6), the self-cyclized thiolactone occurred as the major product (60–90%) at short reaction times (3 hour). However, this species was largely converted to the desired MOrPH after overnight incubation (Fig. 2D and S2†), resulting in estimated MOrPH-to-thiolactone ratios ranging from 1 : 1 to 3 : 1.

Addition of the BPDS oxidizing reagent to the post-cyclization reactions then resulted in the fast and quantitative conversion of the hybrid organo-peptide macrocycles into the corresponding disulfide-bridged bicycles for all nine constructs tested (Fig. 2C–D and S2†). Interestingly, an appreciable decrease (*e.g.* MG10_U + 1 and MG10_U + 5) or even complete disappearance (*e.g.* MG10_U + 2 and MG10_U + 3) of the MS signal corresponding to the self-cyclized product was observed during the oxidation step. These results can be rationalized based on the additional time required for the oxidation step, during which further conversion of the thiolactone into the MOrPH could occur by direct reaction of the former with the synthetic precursor. Altogether, the results obtained with the 10mer constructs described above demonstrated the viability of the present strategy in the context of longer peptide target sequences, thereby enabling the diversification of these

bicyclic scaffolds by varying the length of the peptidic moiety (Fig. S2†).

Bicyclization with alternative synthetic precursors

Finally, further studies were conducted to examine the versatility of this approach toward giving access to bicyclic peptides incorporating different non-peptidic moieties. To this end, the bicyclization of all 16 peptide sequences described in Table 1 with an alternative synthetic precursor, compound **2** (Fig. 1), was investigated. In particular, we were interested in determining whether the more compact structure of **2** (compared to **1**) would have an effect on the relative efficiency by which bicycles encompassing 8- and 10-amino acid long peptide sequences could be obtained. **2**-induced macrocyclization was found, in fact, to maintain the same reactivity trends as observed in the presence of **1**. Specifically, the 8mer constructs with Cys at U + 5/U + 6/U + 7 and the 10mer constructs with Cys at U + 7/U + 8/U + 9, all led to the corresponding **2**-containing MOrPHs as the sole product by 3 hour incubation (Fig. S3 and S4†). As observed with **1**, the remaining constructs displayed a mixture of self-cyclized and MOrPH products, with the yield of the hybrid macrocycle greatly increasing after overnight incubation. The only exceptions were the MG8_U + 1 and MG8_U + 2 constructs, which resulted in poor MOrPH yields (<10%) even after 24 hours. From these results, we infer that the occurrence of the two types of reactivity behaviours exhibited by the cysteine-containing precursor polypeptides is general, *i.e.* it holds true in the presence of different synthetic precursor reagents. Importantly, BPDS-mediated oxidation of the **2**-based MOrPHs was found to proceed rapidly (1 hour) and efficiently (quantitative conversion) for the large majority (14/16) of the constructs tested (Fig. S3 and S4†). Low amounts of the target bicyclic products were detected only for the aforementioned MG8_U + 1 and MG8_U + 2 constructs due to the low MOrPH yields obtained with these precursor sequences during the macrocyclization step. This notwithstanding, these results indicated that the present bicyclization strategy is compatible with the use of different synthetic precursor structures and it could therefore be applied for further diversifying these bicyclic constructs *via* the integration of functionally and structurally different non-peptidic scaffolds (Fig. 3B, S3, S4†).

Conclusions

In summary, we have developed a novel strategy for generating bicyclic organo-peptide hybrids *via* the chemo- and regioselective macrocyclization of ribosomally derived polypeptide precursors followed by intramolecular disulfide bond formation. Our experiments with the 'cysteine scan' series of 8mer and 10mer peptide sequences and two oxyamine/amino-thiol reagents showed that bicyclic scaffolds accommodating peptide moieties of varying length and composition as well as different non-peptidic moieties could be readily and efficiently produced *via* a single-pot, two-step reaction sequence.

Bicyclization has provided a means to improve the binding affinity, target specificity, and/or proteolytic stability of biologically active macrocyclic peptides.[53–56] The remarkable flexibility exhibited by the MOrPH scaffolds with respect to the installation of the second, intramolecular linkage holds promise toward exploiting the bicyclization methodology described here for improving the properties of this new class of hybrid macrocycles. This feature is also expected to make this strategy valuable toward providing access to diverse, combinatorial libraries of bicyclic ligands for screening purposes. In particular, the unique structural space covered by these scaffolds is expected to expand the portfolio of natural product-inspired macrocycles[19,20] which could be exploited to probe challenging biomolecular interactions.

Experimental

Cloning

Oligonucleotides were purchased from Integrated DNA technologies and their sequences are provided in Table S1 of the ESI†. PCR reactions with forward primers 8mer C@U + 4, 8mer C@U + 5, 8mer C@U + 6, 8mer C@U + 7 and primer T7_terminator were carried out to amplify the respective 8mer-GyrA constructs. For such constructs, the template was pMG_G8T, a pET22b-based plasmid encoding for MG(amber stop)TGSAEYGT peptide, followed by *Mxe* GyrA(N198A) and a His tag. The PCR products (~0.75 kbp) were digested with *BamH* I and *Xho* I and cloned into the pMG-G8 T vector to produce pMG8_U + 4, pMG8_U + 5, pMG8_U + 6, and pMG8_U + 7. Vectors for the expression of MG10_U + 4, MG10_U + 5, MG10_U + 6, MG10_U + 7, MG10_U + 8, and MG10_U + 9 were prepared in a similar manner. Genes encoding MG8_U + 1, MG8_U + 2, and MG8_U + 3 were PCR amplified using the primers 8/10mer C@U + 1, 8mer C@U + 2, and 8mer C@U + 3, digested with *Nde* I and *Xho* I, and cloned into pMG-G8 T. Vectors for the expression of MG10_U + 1, MG10_U + 2, and MG10_U + 3 were prepared in a similar manner. In all the plasmids above, the gene encoding for the biosynthetic precursor protein is under the control of an IPTG-inducible T7 promoter. All the plasmid constructs were confirmed by DNA sequencing. A pEVOL-based vector for the expression of engineered *Methanococcus jannaschii* $tRNA_{CUA}$ and aminoacyl-tRNA synthetase (*Mj*TyrRS) for amber codon suppression with *para*-acetylphenylalanine (pAcF)[50] was kindly provided by the Schultz group.

Protein expression and purification

To express the pAcF-containing biosynthetic precursors, pEVOL_pAcF and the pET22-based vector encoding for appropriate biosynthetic precursor were co-transformed into BL21 (DE3) *E. coli* cells. Overnight cultures were grown in Luria-Bertani (LB) media containing ampicillin (50 mg L^{-1}) and chloramphenicol (34 mg L^{-1}) and used to inoculate a 0.2 L M9 media containing ampicillin (50 mg L^{-1}), chloramphenicol (34 mg L^{-1}), 1% glycerol, and 1% (w/v) yeast extract. At an OD_{600} of 0.6, cultures were added with L-arabinose (0.08%

w/v), pAcF (2 mM), and IPTG (0.5 mM). After overnight incubation at 27 °C, cells were harvested by centrifugation and resuspended in 50 mM Tris, 300 mM NaCl, 20 mM imidazole buffer (pH 7.4). Cells were then lysed by sonication. The clarified lysates were loaded onto a Ni-NTA affinity column and the protein was eluted with 50 mM Tris, 150 mM NaCl, 300 mM imidazole (pH 7.4). After buffer exchange with potassium phosphate 50 mM, NaCl 150 mM buffer (pH 7.5), aliquots of the protein solutions were stored at −80 °C. Protein concentration was determined using the extinction coefficient at 280 nm (ε_{280}) calculated based on the protein primary sequence. Typical expression yields for the pAcF-containing biosynthetic precursors were 30–40 mg L^{-1} culture. The identity of the isolated proteins was confirmed by MALDI-TOF and SDS-PAGE.

Synthesis of synthetic precursors

Compounds **1** and **2** were synthesized starting from methyl 3-amino-4-methylbenzoate as described previously.[37]

Macro- and bicyclization reactions

For the macrocyclization reactions, a 100 μL solution of the protein (100 μM) in potassium phosphate buffer (50 mM, NaCl 150 mM, pH 7.5) was added with either **1** or **2** (10 mM) and TCEP (10 mM). After overnight incubation at room temperature, 2,2′-bispyridyl disulfide (BPDS, Sigma-Aldrich) at 10 mM was added to the samples. Small aliquots were withdrawn at different time points during the macrocyclization and oxidation step for MS analysis as described below.

Mass spectrometry analysis

MALDI-TOF analyses were carried out on a Bruker Autoflex III MALDI-TOF spectrometer. Prior to analysis, protein samples were diluted in 70% acetonitrile in H_2O (0.1% TFA) and this solution mixed with a α-cyano-4-hydroxycinnamic acid solution (10 mg mL^{-1} in 70% acetonitrile in H_2O, 0.1% TFA). Product masses were determined using reflectron positive (RP) mode. LC-MS analyses were carried out using an Accela HPLC system coupled to a LTQ Velos ESI-IT mass spectrometer (Thermo Scientific, Runcorn, UK). For LC-MS analyses, chromatographic separations were performed using a 100 × 4.6 mm Vydac TP 3 μm C4 column (Grace) with the column maintained at 25 °C, a binary mobile phase system consisting of A: water + 0.1% formic acid and B: acetonitrile + 0.1% formic acid, a linear gradient from 5 to 95% of B (12 min), and a flow rate of 0.5 mL min^{-1}.

Acknowledgements

This work was supported by the U.S. National Science Foundation grant CHE-1112342 awarded to R.F. J.M.S. was supported by a NSF Graduate Research Fellowship. N.C.H. and P.J.K. acknowledge the NSF REU program for financial support. MS instrumentation was supported by the U.S. National Science Foundation grants CHE-0840410 and CHE-0946653.

Notes and references

1 C. J. White and A. K. Yudin, *Nat. Chem.*, 2011, **3**, 509.
2 T. Satoh, S. Li, T. M. Friedman, R. Wiaderkiewicz, R. Korngold and Z. Huang, *Biochem. Biophys. Res. Commun.*, 1996, **224**, 438.
3 D. P. Fairlie, J. D. A. Tyndall, R. C. Reid, A. K. Wong, G. Abbenante, M. J. Scanlon, D. R. March, D. A. Bergman, C. L. L. Chai and B. A. Burkett, *J. Med. Chem.*, 2000, **43**, 1271.
4 D. Wang, W. Liao and P. S. Arora, *Angew. Chem., Int. Ed.*, 2005, **44**, 6525.
5 O. S. Gudmundsson, D. G. Vander Velde, S. D. Jois, A. Bak, T. J. Siahaan and R. T. Borchardt, *J. Pept. Res.*, 1999, **53**, 403.
6 L. D. Walensky, A. L. Kung, I. Escher, T. J. Malia, S. Barbuto, R. D. Wright, G. Wagner, G. L. Verdine and S. J. Korsmeyer, *Science*, 2004, **305**, 1466.
7 T. Rezai, B. Yu, G. L. Millhauser, M. P. Jacobson and R. S. Lokey, *J. Am. Chem. Soc.*, 2006, **128**, 2510.
8 F. Al-Obeidi, A. M. Castrucci, M. E. Hadley and V. J. Hruby, *J. Med. Chem.*, 1989, **32**, 2555.
9 Y. Q. Tang, J. Yuan, G. Osapay, K. Osapay, D. Tran, C. J. Miller, A. J. Ouellette and M. E. Selsted, *Science*, 1999, **286**, 498.
10 M. A. Dechantsreiter, E. Planker, B. Matha, E. Lohof, G. Holzemann, A. Jonczyk, S. L. Goodman and H. Kessler, *J. Med. Chem.*, 1999, **42**, 3033.
11 N. R. Graciani, K. Y. Tsang, S. L. McCutchen and J. W. Kelly, *Bioorg. Med. Chem.*, 1994, **2**, 999.
12 R. Fasan, R. L. Dias, K. Moehle, O. Zerbe, J. W. Vrijbloed, D. Obrecht and J. A. Robinson, *Angew. Chem., Int. Ed.*, 2004, **43**, 2109.
13 R. M. Cardoso, F. M. Brunel, S. Ferguson, M. Zwick, D. R. Burton, P. E. Dawson and I. A. Wilson, *J. Mol. Biol.*, 2007, **365**, 1533.
14 L. K. Henchey, J. R. Porter, I. Ghosh and P. S. Arora, *ChemBioChem*, 2010, **11**, 2104.
15 L. A. Wessjohann, E. Ruijter, D. Garcia-Rivera and W. Brandt, *Mol. Divers.*, 2005, **9**, 171.
16 E. M. Driggers, S. P. Hale, J. Lee and N. K. Terrett, *Nat. Rev. Drug Discovery.*, 2008, **7**, 608.
17 J. A. Robinson, S. Demarco, F. Gombert, K. Moehle and D. Obrecht, *Drug Discovery Today*, 2008, **13**, 944.
18 E. Marsault and M. L. Peterson, *J. Med. Chem.*, 2011, **54**, 1961.
19 J. M. Smith, J. R. Frost and R. Fasan, *J. Org. Chem.*, 2013, **78**, 3525.
20 J. R. Frost, J. M. Smith and R. Fasan, *Curr. Opin. Struct. Biol.*, 2013, **23**, 571.
21 C. P. Scott, E. Abel-Santos, M. Wall, D. C. Wahnon and S. J. Benkovic, *Proc. Natl. Acad. Sci. U. S. A.*, 1999, **96**, 13638.
22 A. Tavassoli and S. J. Benkovic, *Nat. Protoc.*, 2007, **2**, 1126.
23 S. W. Millward, T. T. Takahashi and R. W. Roberts, *J. Am. Chem. Soc.*, 2005, **127**, 14142.

24 C. Heinis, T. Rutherford, S. Freund and G. Winter, *Nat. Chem. Biol.*, 2009, **5**, 502.
25 Y. V. G. Schlippe, M. C. T. Hartman, K. Josephson and J. W. Szostak, *J. Am. Chem. Soc.*, 2012, **134**, 10469.
26 C. J. Hipolito and H. Suga, *Curr. Opin. Chem. Biol.*, 2012, **16**, 196.
27 F. T. Hofmann, J. W. Szostak and F. P. Seebeck, *J. Am. Chem. Soc.*, 2012, **134**, 8038.
28 M. R. Levengood, P. J. Knerr, T. J. Oman and W. A. van der Donk, *J. Am. Chem. Soc.*, 2009, **131**, 12024.
29 F. Oldach, R. Al Toma, A. Kuthning, T. Caetano, S. Mendo, N. Budisa and R. D. Sussmuth, *Angew. Chem., Int. Ed.*, 2012, **51**, 415.
30 M. D. Tianero, M. S. Donia, T. S. Young, P. G. Schultz and E. W. Schmidt, *J. Am. Chem. Soc.*, 2012, **134**, 418.
31 T. S. Young, P. C. Dorrestein and C. T. Walsh, *Chem. Biol.*, 2012, **19**, 1600.
32 M. O. Maksimov, S. J. Pan and A. J. Link, *Nat. Prod. Rep.*, 2012, **29**, 996.
33 D. J. Craik and A. C. Conibear, *J. Org. Chem.*, 2011, **76**, 4805.
34 H. Sancheti and J. A. Camarero, *Adv. Drug Delivery Rev.*, 2009, **61**, 908.
35 J. M. Smith, F. Vitali, S. A. Archer and R. Fasan, *Angew. Chem., Int. Ed.*, 2011, **50**, 5075.
36 M. Satyanarayana, F. Vitali, J. R. Frost and R. Fasan, *Chem. Commun.*, 2012, **48**, 1461.
37 J. R. Frost, F. Vitali, N. T. Jacob, M. D. Brown and R. Fasan, *ChemBioChem*, 2013, **14**, 147.
38 N. H. Tan and J. Zhou, *Chem. Rev.*, 2006, **106**, 840.
39 D. J. Craik, N. L. Daly, T. Bond and C. Waine, *J. Mol. Biol.*, 1999, **294**, 1327.
40 J. E. Velasquez and W. A. van der Donk, *Curr. Opin. Chem. Biol.*, 2011, **15**, 11.
41 Y. Sun, G. S. Lu and J. P. Tam, *Org. Lett.*, 2001, **3**, 1681.
42 W. D. Kohn, L. S. Zhang and J. A. Weigel, *Org. Lett.*, 2001, **3**, 971.
43 J. Ruiz-Rodriguez, J. Spengler and F. Albericio, *Angew. Chem., Int. Ed.*, 2009, **48**, 8564.
44 M. Bartoloni, R. U. Kadam, J. Schwartz, J. Furrer, T. Darbre and J. L. Reymond, *Chem. Commun.*, 2011, **47**, 12634.
45 B. K. W. Chung, J. L. Hickey, C. C. G. Scully, S. Zaretsky and A. K. Yudin, *MedChemComm*, 2013, **4**, 1124.
46 T. Karskela, P. Virta and H. Lonnberg, *Curr. Org. Synth.*, 2006, **3**, 283.
47 Y. Sako, J. Morimoto, H. Murakami and H. Suga, *J. Am. Chem. Soc.*, 2008, **130**, 7232.
48 K. Iwasaki, Y. Goto, T. Katoh and H. Suga, *Org. Biomol. Chem.*, 2012, **10**, 5783.
49 I. R. Rebollo, A. Angelini and C. Heinis, *MedChemComm*, 2013, **4**, 145.
50 L. Wang, Z. Zhang, A. Brock and P. G. Schultz, *Proc. Natl. Acad. Sci. U. S. A.*, 2003, **100**, 56.
51 J. C. Collins and K. James, *MedChemComm*, 2012, **3**, 1489.
52 K. Maruyama, H. Nagasawa and A. Suzuki, *Peptides*, 1999, **20**, 881.
53 D. D. Smith, J. Slaninova and V. J. Hruby, *J. Med. Chem.*, 1992, **35**, 1558.
54 R. L. Dias, R. Fasan, K. Moehle, A. Renard, D. Obrecht and J. A. Robinson, *J. Am. Chem. Soc.*, 2006, **128**, 2726.
55 J. S. Quartararo, P. Wu and J. A. Kritzer, *ChemBioChem*, 2012, **13**, 1490.
56 W. Lian, P. Upadhyaya, C. A. Rhodes, Y. Liu and D. Pei, *J. Am. Chem. Soc.*, 2013, **135**, 11990.

Supplemental Information for

Synthesis of bicyclic organo-peptide hybrids via oxime/intein-mediated macrocyclization followed by disulfide bond formation

Jessica M. Smith, Nicholas C. Hill, Peter J. Krasniak, and Rudi Fasan*

[1]*Department of Chemistry, University of Rochester, Rochester, New York 14627, USA.*

*fasan@chem.rochester.edu

Table of Contents:

Supplementary Table S1: Oligonucleotide primers

Primer	Sequence
8/10mer(C@U+1)_for	5'-GCATCCCATGGCTAGTGCGGATCC-3'
8mer(C@U+2)_for	5'-GCATCCCATGGCTAGACATGCTCCGCC-3'
8mer(C@U+3)_for	5'-GCATCCCATGGCTAGACAGGATGCGCCGA-3'
8mer(C@U+4)_for	5'-CCACAGGATCCTGCGAATACGGCACC-3'
8mer(C@U+5)_for	5'-CCACAGGATCCGCCTGCTACGGCACC-3'
8mer(C@U+6)_for	5'-CCACAGGATCCGCCGAATGCGGCACC-3'
8mer(C@U+7)_for	5'-CCACAGGATCCGCCGAATACTGCACCTG-3'
10mer(C@U+2)_for	5'-GCATCCCATGGCTAGACATGCTCCAAACTG-3'
10mer(C@U+3)_for	5'-GCATCCCATGGCTAGACAGGATGCAAACTG-3'
10mer(C@U+4)_for	5'-CAACAGGATCCTGCCTGGCCGAATACGG-3'
10mer(C@U+5)_for	5'-CAACAGGATCCAAATGCGCCGAATACGG-3'
10mer(C@U+6)_for	5'-CAACAGGATCCAAACTGTGCGAATACGG-3'
10mer(C@U+7)_for	5'-CAACAGGATCCAAACTGGCCTGCTACGG-3'
10mer(C@U+8)_for	5'-CAACAGGATCCAAACTGGCCGAATGCGG-3'
10mer(C@U+9)_for	5'-CAACAGGATCCAAACTGGCCGAATACTGCACCTG-3'
T7 terminator primer	5'-GCTAGTTATTGCTCAGCGG-3'
T7_term_long	5'-GCTAGTTATTGCTCAGCGGTGGC-3'

Supplementary Figure S1. MALDI-TOF MS analysis of the reactions between **1** (SP6) and the 8mer biosynthetic precursors (MG8 series, Table 1). Spectra correspond to the three hour (*left*) and 24 hour time point (*center*) after addition of **1** and one hour time point after addition of BPDS (*right*). Peaks corresponding to the proton ($[M+H]^+$), sodium ($[M+Na]^+$), and potassium ($[M+K]^+$) adducts of the MOrPH ('m'), self-cyclized thiolactone ('sc') and bicyclic product ('b') are labeled. When no self-cyclized product is formed, the 24 hr-time point spectrum is omitted as it is identical to the 3-hr spectrum. The calculated and observed *m/z* values for the proton (or sodium) adducts are provided in the table. The structure of the bicyclic product is also shown.

MG8_U+1 / SP6 (3h) **MG8_U+1 / SP6 (24h)** **MG8_U+1 / SP6 (post-oxidation)**

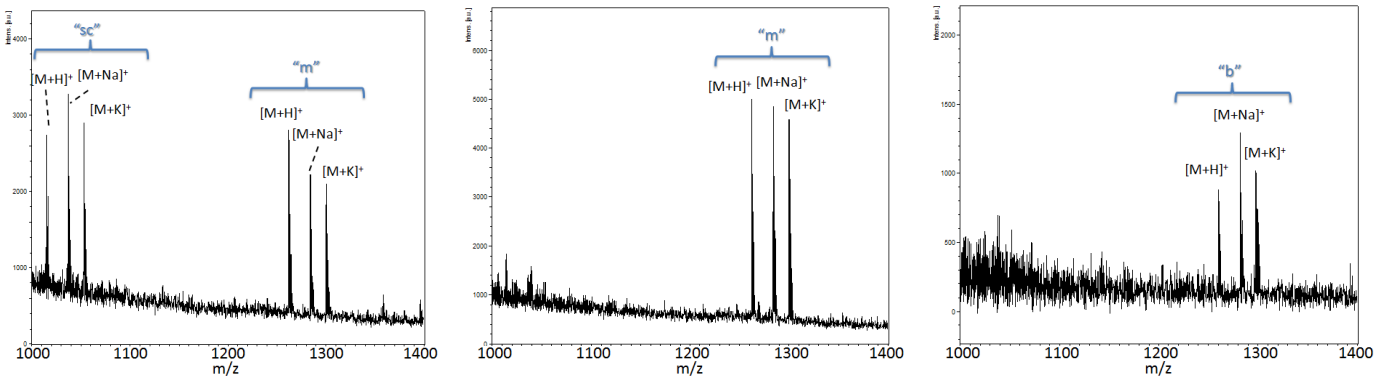

MG8_U+1 and SP6	Calc $[M+H]^+$	Obs $[M+H]^+$
MOrPH ("m")	1263.4	1262.8
Thiolactone ("sc")	1016.1	1015.7
Bicycle ("b")	1261.4	1260.7

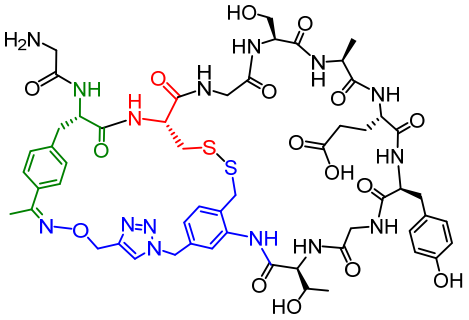

MG8_U+2 / SP6 (3h)

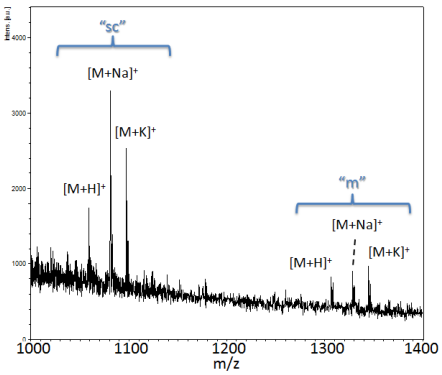

MG8_U+2 / SP6 (24h)

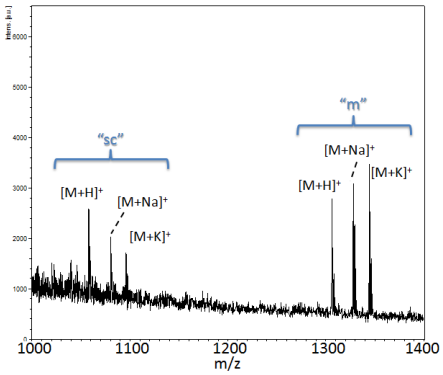

MG8_U+2 / SP6 (post-oxidation)

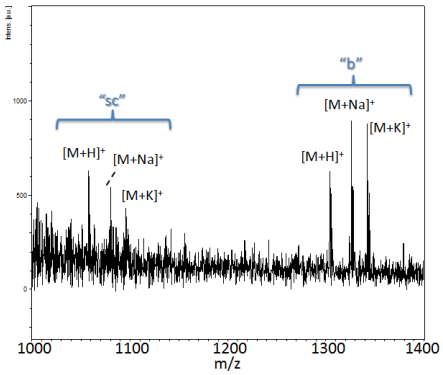

MG8_U+2 and SP6	Calc $[M+H]^+$	Obs $[M+H]^+$
MOrPH ("m")	1307.5	1306.9
Thiolactone ("sc")	1060.2	1059.8
Bicycle ("b")	1305.5	1304.9

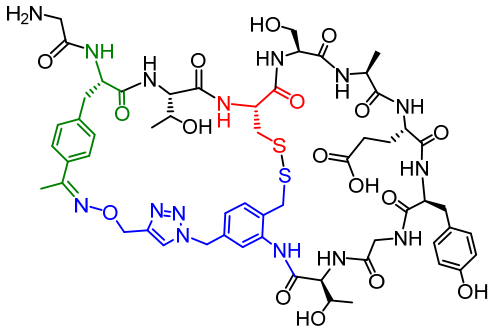

MG8_U+3 / SP6 (3h)

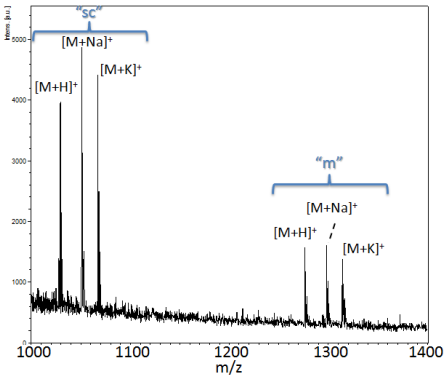

MG8_U+3 / SP6 (24h)

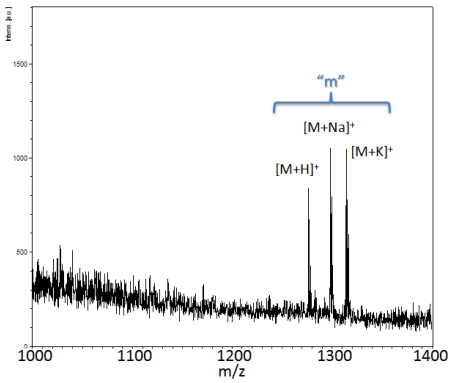

MG8_U+3 / SP6 (post-oxidation)

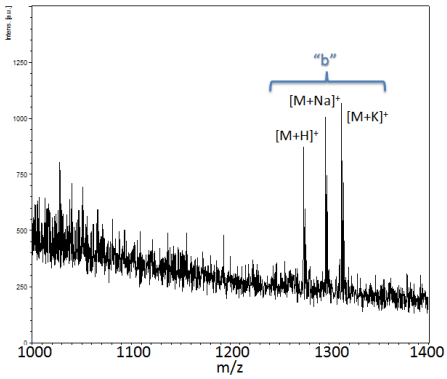

MG8_U+3 and SP6	Calc $[M+H]^+$	Obs $[M+H]^+$
MOrPH ("m")	1277.5	1276.7
Thiolactone ("sc")	1030.2	1029.6
Bicycle ("b")	1275.5	1274.7

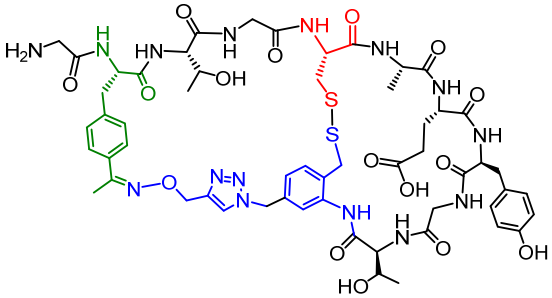

MG8_U+4 / SP6 (3h)

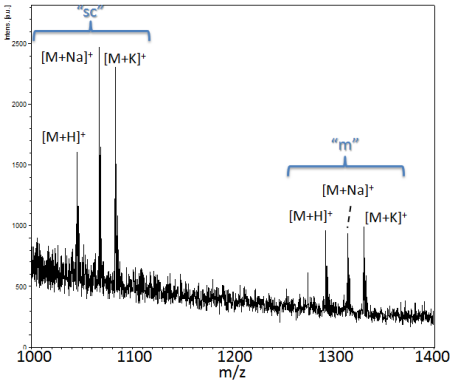

MG8_U+4 / SP6 (24h)

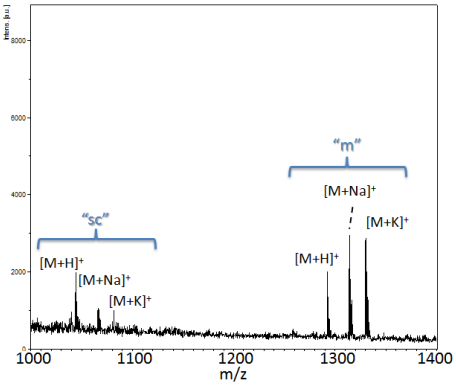

MG8_U+4 / SP6 (post-oxidation)

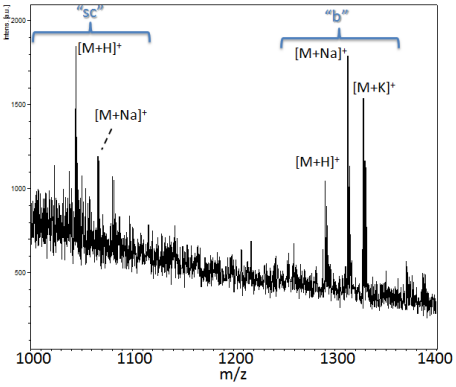

MG8_U+4 and SP6	Calc $[M+H]^+$	Obs $[M+H]^+$
MOrPH ("m")	1293.5	1292.8
Thiolactone ("sc")	1046.2	1045.8
Bicycle ("b")	1291.5	1290.8

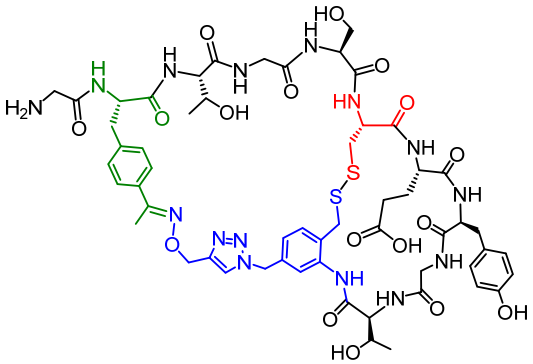

MG8_U+5 / SP6 (3h)

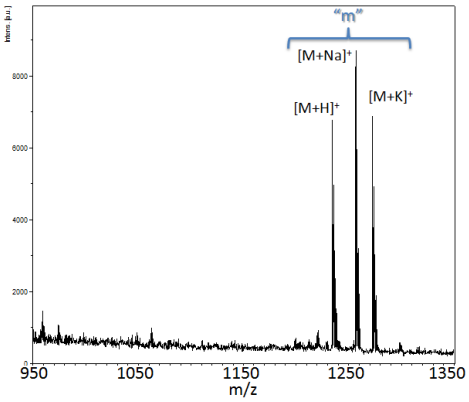

MG8_U+5 / SP6 (post-oxidation)

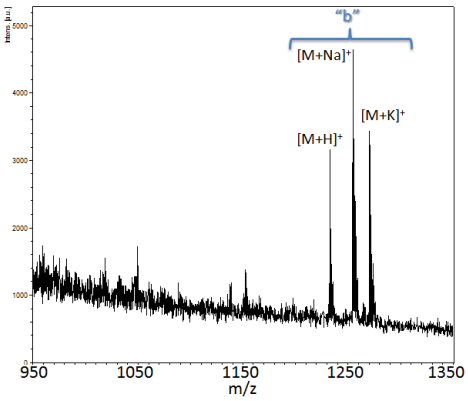

MG8_U+5 and SP6	Calc $[M+H]^+$	Obs $[M+H]^+$
MOrPH ("m")	1235.4	1234.7
Thiolactone ("sc")	988.1	not obs.
Bicycle ("b")	1233.4	1232.6

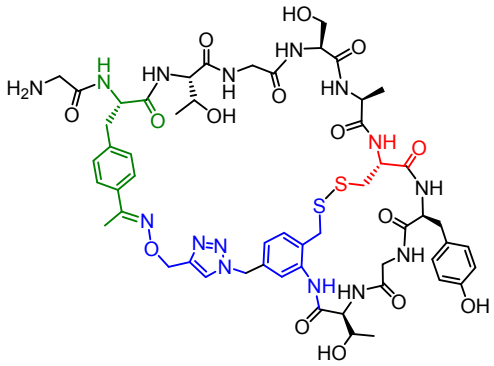

MG8_U+6 / SP6 (3h)

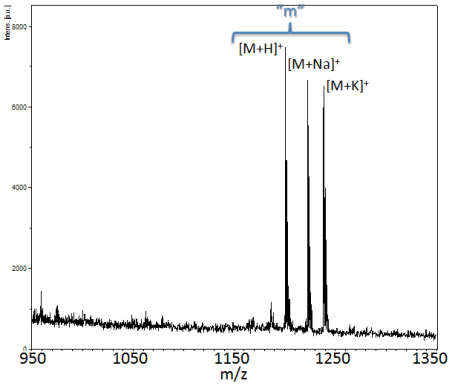

MG8_U+6 / SP6 (post-oxidation)

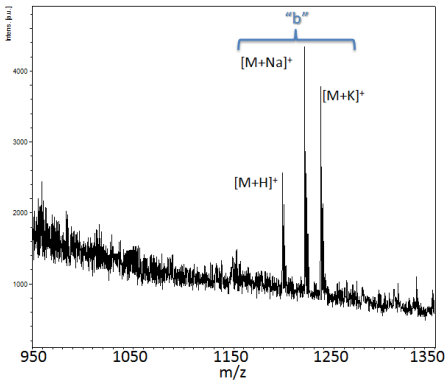

MG8_U+6 and SP6	Calc $[M+H]^+$	Obs $[M+H]^+$
MOrPH ("m")	1201.4	1200.7
Thiolactone ("sc")	954.1	not obs.
Bicycle ("b")	1199.4	1198.7

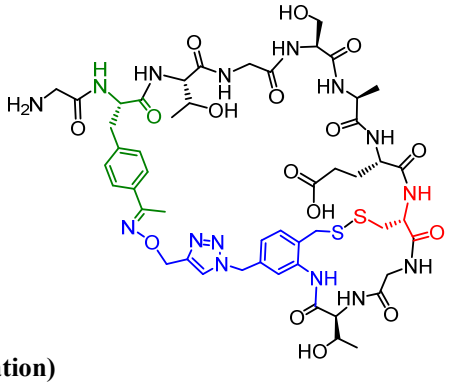

MG8_U+7 / SP6 (3h)

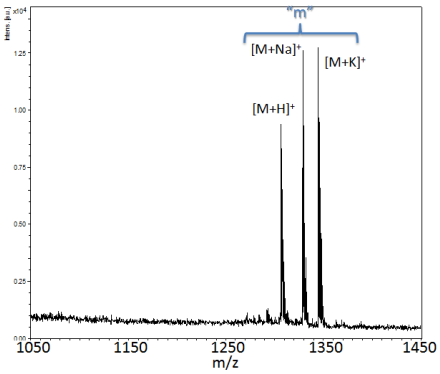

MG8_U+7 / SP6 (post-oxidation)

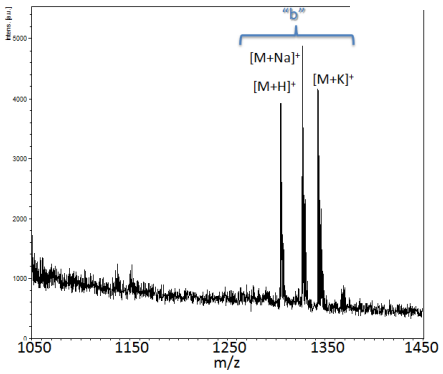

MG8_U+7 and SP6	Calc $[M+H]^+$	Obs $[M+H]^+$
MOrPH ("m")	1307.5	1306.8
Thiolactone ("sc")	1060.2	not obs.
Bicycle ("b")	1305.5	1304.8

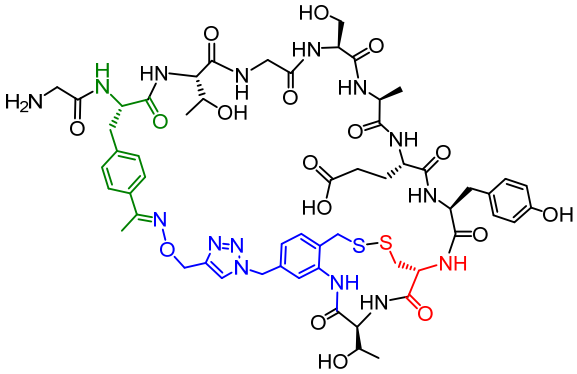

Supplementary Figure S2. MALDI-TOF MS analysis of the reactions between **1** (SP6) and the 10mer biosynthetic precursors (MG10 series, Table 1). Spectra correspond to the three hour (*left*) and 24 hour time point (*center*) after addition of **1** and one hour time point after addition of BPDS (*right*). Peaks corresponding to the proton ($[M+H]^+$), sodium ($[M+Na]^+$), and potassium ($[M+K]^+$) adducts of the MOrPH ('m'), self-cyclized thiolactone ('sc') and bicyclic product ('b') are labeled. When no self-cyclized product is formed, the 24 hr-time point spectrum is omitted as it is identical to the 3-hr spectrum. The calculated and observed *m/z* values for the proton (or sodium) adducts are provided in the table. The structure of the bicyclic product is also shown.

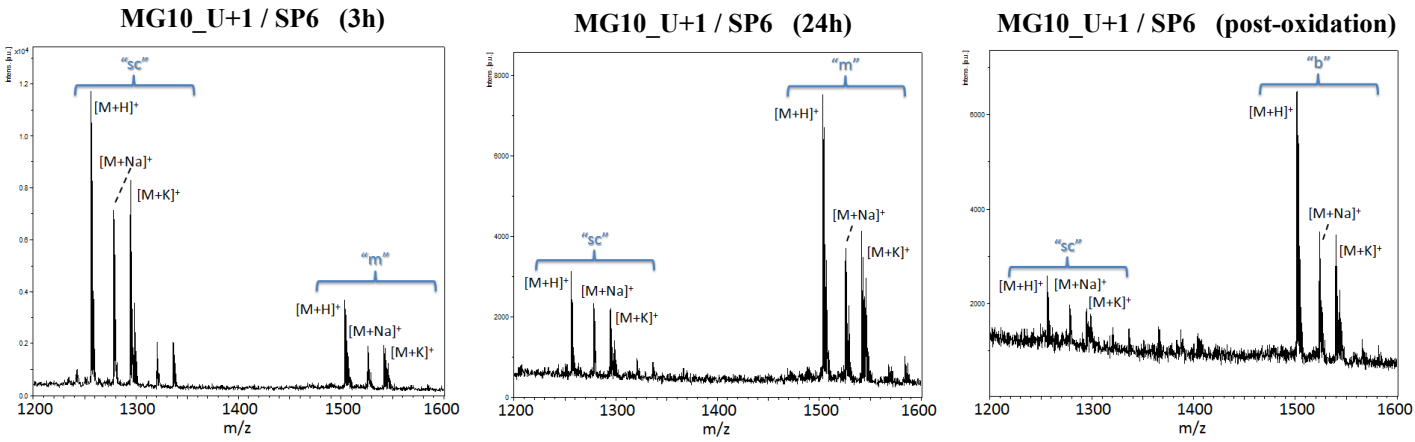

MG10_U+1 and SP6	Calc $[M+H]^+$	Obs $[M+H]^+$
MOrPH ("m")	1504.6	1504.1
Thiolactone ("sc")	1257.3	1256.9
Bicycle ("b")	1502.6	1502.1

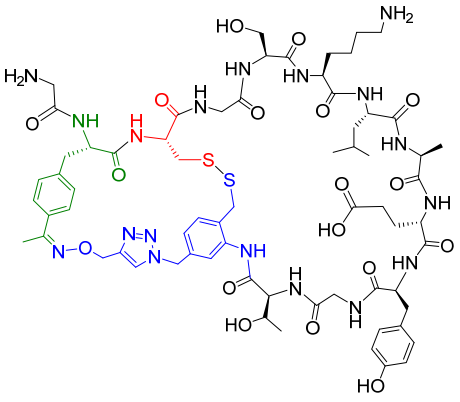

MG10_U+2 / SP6 (3h)

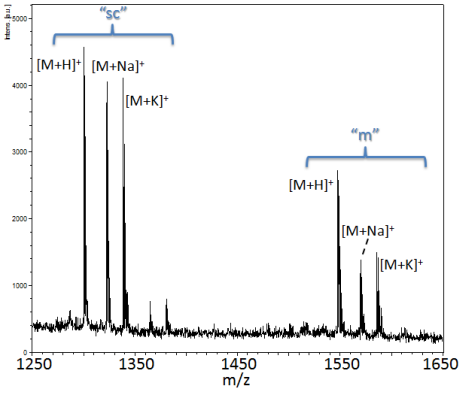

MG10_U+2 / SP6 (24h)

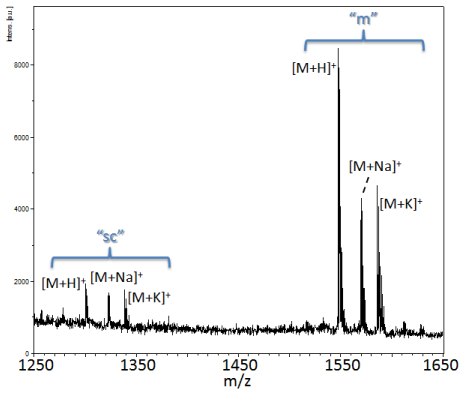

MG10_U+2 / SP6 (post-oxidation)

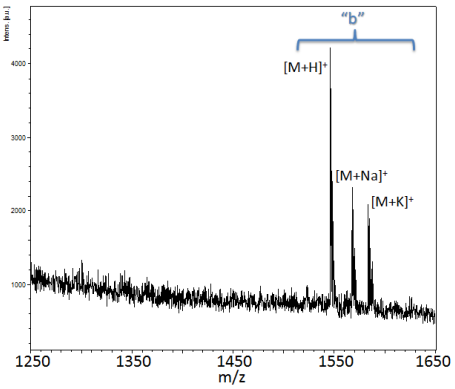

MG10_U+2 and SP6	Calc $[M+H]^+$	Obs $[M+H]^+$
MOrPH ("m")	1504.6	1503.9
Thiolactone ("sc")	1257.3	1256.8
Bicycle ("b")	1502.6	1501.9

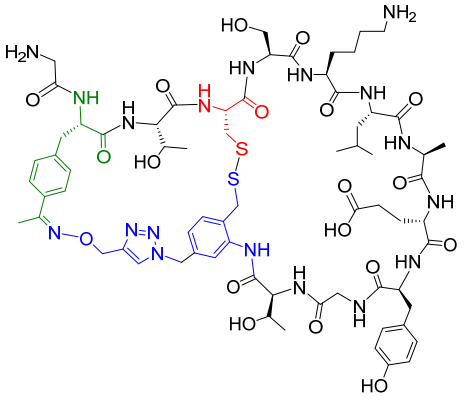

MG10_U+3 / SP6 (3h)

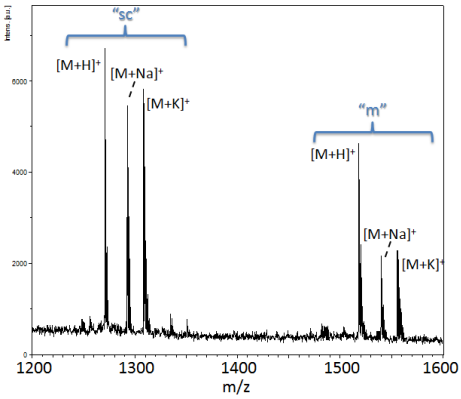

MG10_U+3 / SP6 (24h)

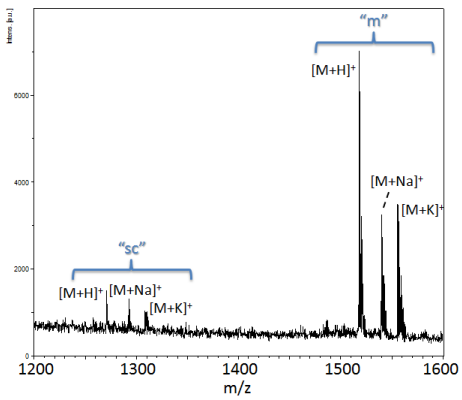

MG10_U+3 / SP6 (post-oxidation)

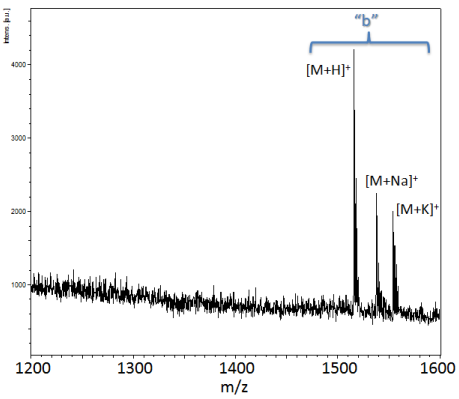

MG10_U+3 and SP6	Calc $[M+H]^+$	Obs $[M+H]^+$
MOrPH ("m")	1518.7	1517.9
Thiolactone ("sc")	1271.4	1270.8
Bicycle ("b")	1516.7	1515.9

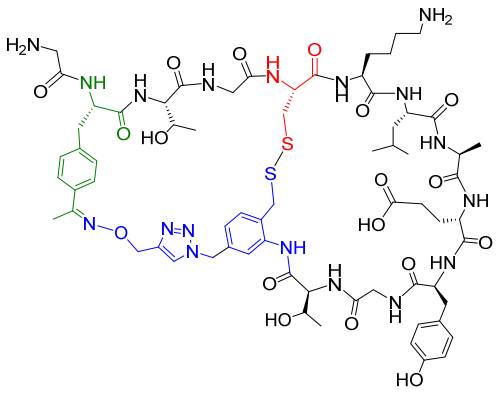

MG10_U+4 / SP6 (3h)

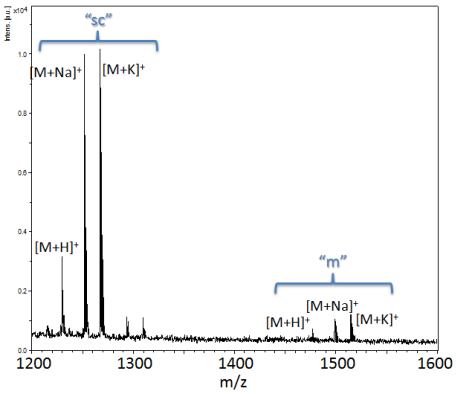

MG10_U+4 / SP6 (24h)

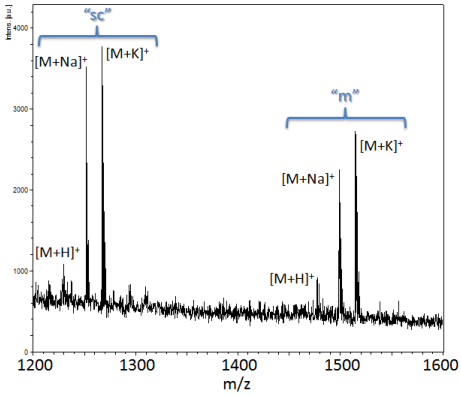

MG10_U+4 / SP6 (post-oxidation)

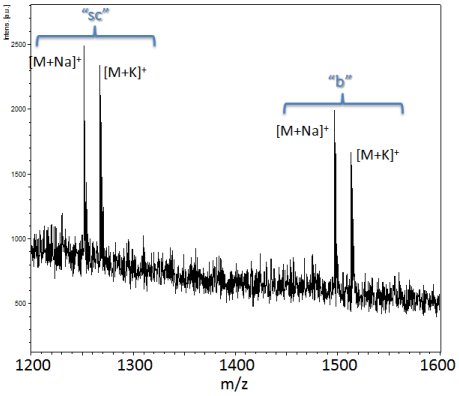

MG10_U+4 and SP6	Calc $[M+Na]^+$	Obs $[M+Na]^+$
MOrPH ("m")	1499.7	1498.9
Thiolactone ("sc")	1252.4	1251.8
Bicycle ("b")	1497.7	1496.9

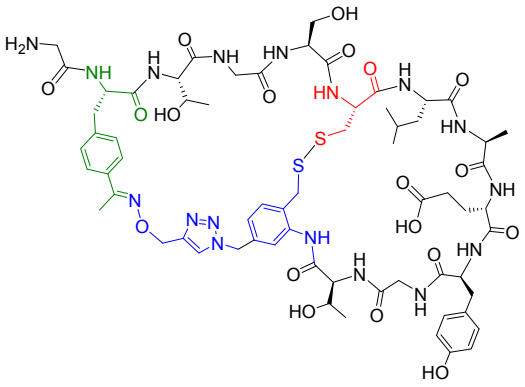

MG10_U+5 / SP6 (3h)

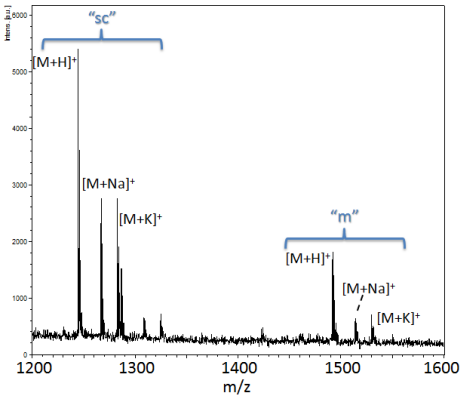

MG10_U+5 / SP6 (24h)

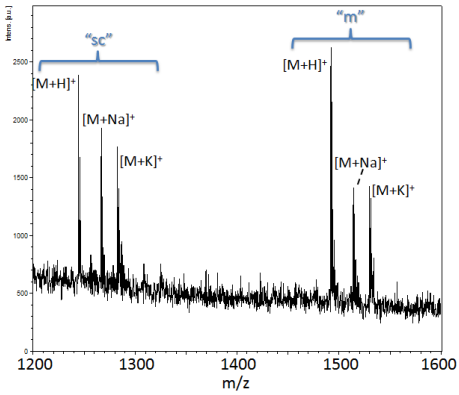

MG10_U+5 / SP6 (post-oxidation)

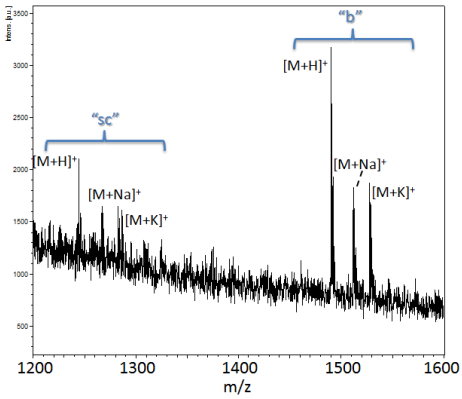

MG10_U+5 and SP6	Calc $[M+H]^+$	Obs $[M+H]^+$
MOrPH ("m")	1492.7	1492.0
Thiolactone ("sc")	1245.4	1244.8
Bicycle ("b")	1490.7	1489.9

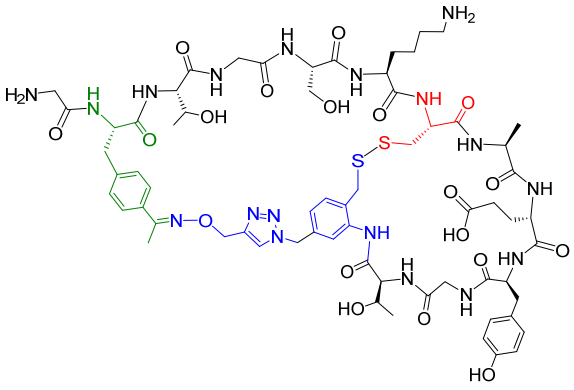

MG10_U+6 / SP6 (3h)

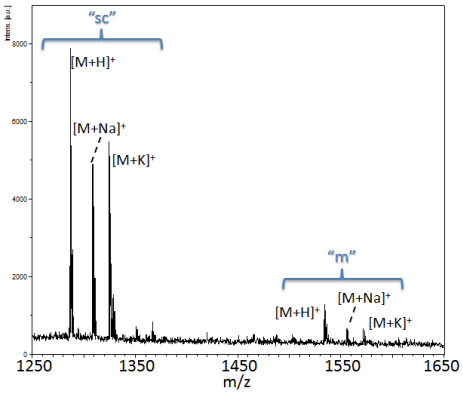

MG10_U+6 / SP6 (24h)

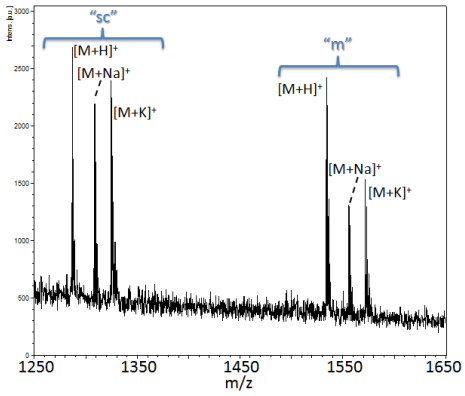

MG10_U+6 / SP6 (post-oxidation)

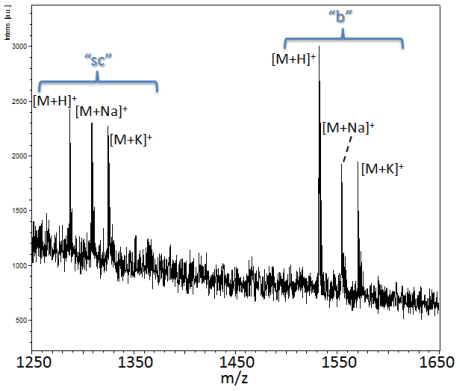

MG10_U+6 and SP6	Calc $[M+H]^+$	Obs $[M+H]^+$
MOrPH ("m")	1534.8	1534.1
Thiolactone ("sc")	1287.5	1286.9
Bicycle ("b")	1532.8	1532.1

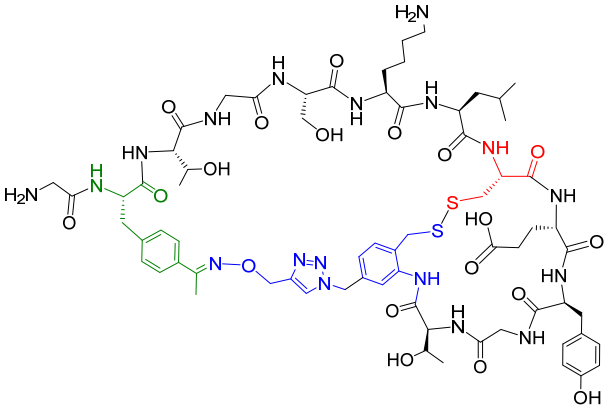

MG10_U+7 / SP6 (3h)

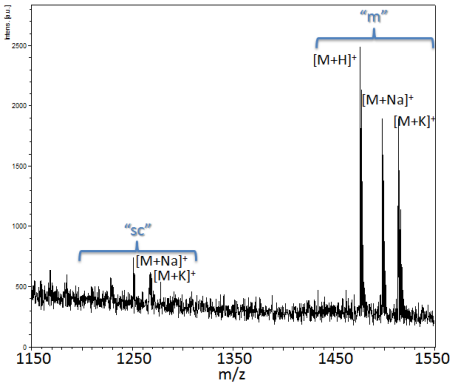

MG10_U+7 / SP6 (post-oxidation)

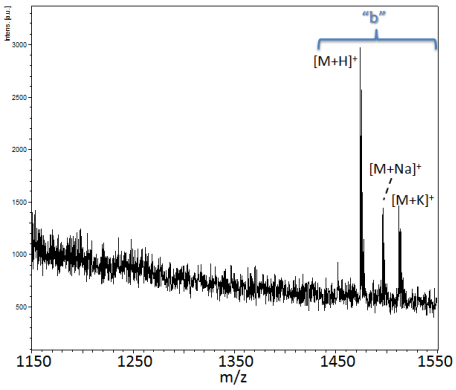

MG10_U+7 and SP6	Calc $[M+Na]^+$	Obs $[M+Na]^+$
MOrPH ("m")	1498.8	1498.1
Thiolactone ("sc")	1251.5	1250.9
Bicycle ("b")	1496.8	1496.1

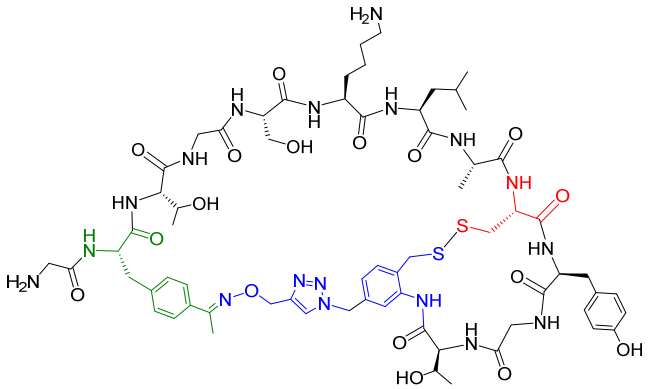

MG10_U+8 / SP6 (3h)

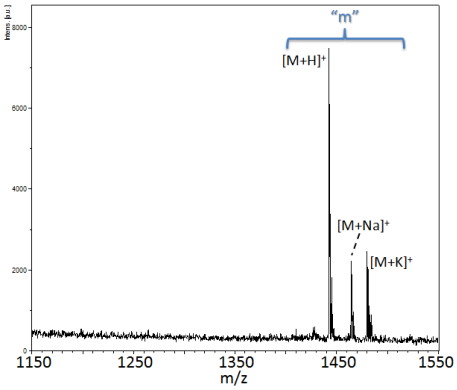

MG10_U+8 / SP6 (post-oxidation)

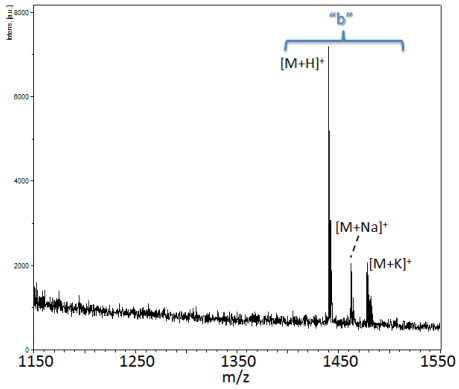

MG10_U+8 and SP6	Calc $[M+H]^+$	Obs $[M+H]^+$
MOrPH ("m")	1442.7	1442.1
Thiolactone ("sc")	1195.4	n/o
Bicycle ("b")	1440.7	1440.1

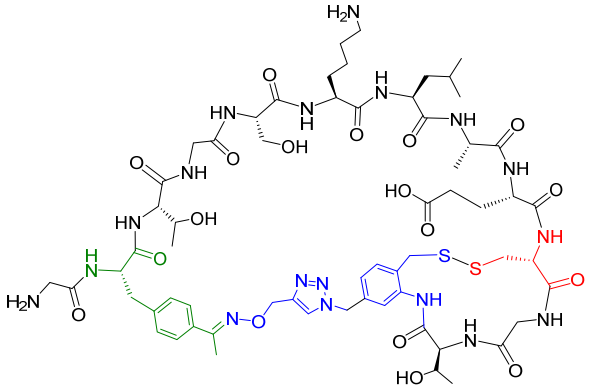

MG10_U+9 / SP6 (3h)

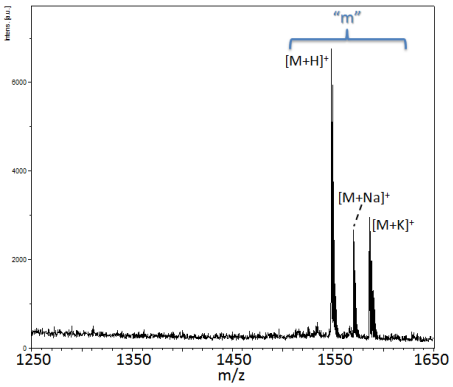

MG10_U+9 / SP6 (post-oxidation)

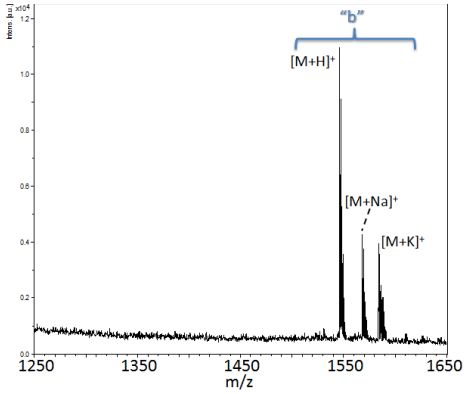

MG10_U+9 and SP6	Calc $[M+H]^+$	Obs $[M+H]^+$
MOrPH ("m")	1548.8	1548.2
Thiolactone ("sc")	1301.5	n/o
Bicycle ("b")	1546.8	1546.2

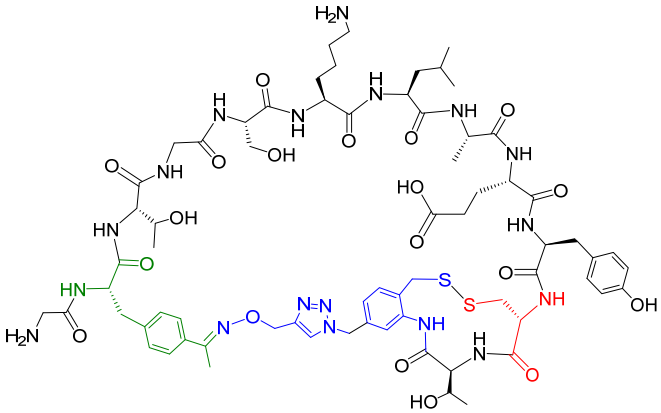

Supplementary Figure S3. MALDI-TOF MS analysis of the reactions between **2** (SP4) and the 8mer biosynthetic precursors (MG8 series, Table 1). Spectra correspond to the three hour (*left*) and 24 hour time point (*center*) after addition of **1** and one hour time point after addition of BPDS (*right*). Peaks corresponding to the proton ($[M+H]^+$), sodium ($[M+Na]^+$), and potassium ($[M+K]^+$) adducts of the MOrPH ('m'), self-cyclized thiolactone ('sc') and bicyclic product ('b') are labeled. When no self-cyclized product is formed, the 24 hr-time point spectrum is omitted as it is identical to the 3-hr spectrum. The calculated and observed *m/z* values for the proton (or sodium) adducts are provided in the table. The structure of the bicyclic product is also shown.

MG8_U+1 / SP4 (3h)

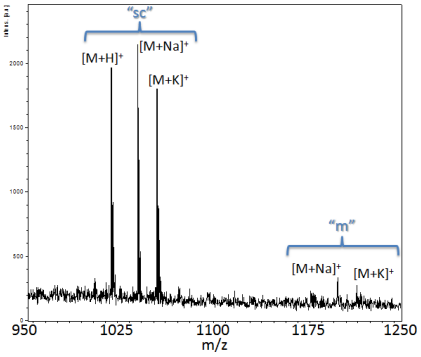

MG8_U+1 / SP4 (24h)

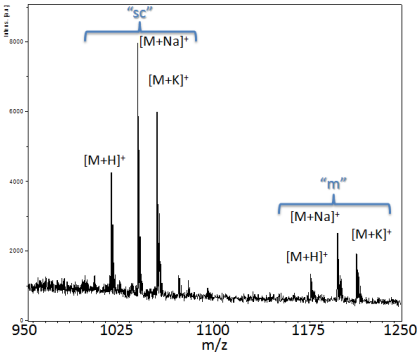

MG8_U+1 / SP4 (post-oxidation)

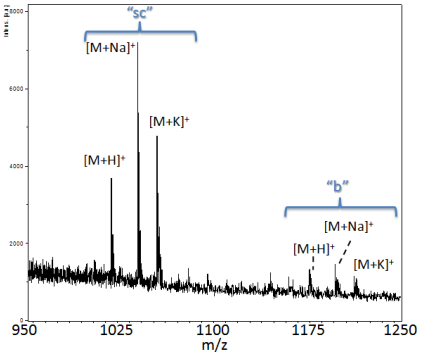

MG8_U+1 and SP4	Calc $[M+H]^+$	Obs $[M+H]^+$
MOrPH ("m")	1182.4	1181.6
Thiolactone ("sc")	1016.1	1015.6
Bicycle ("b")	1180.4	1179.8

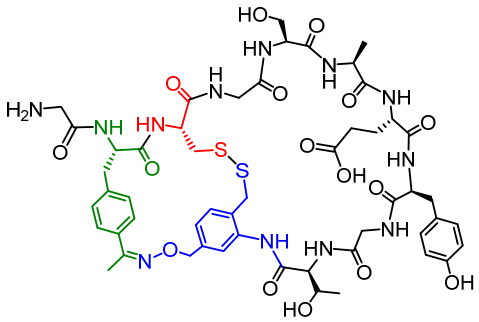

MG8_U+2 / SP4 (3h)

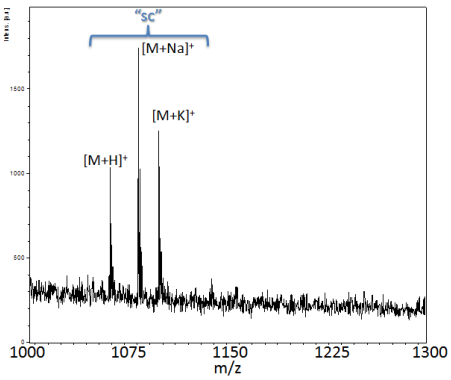

MG8_U+2 / SP4 (3h)

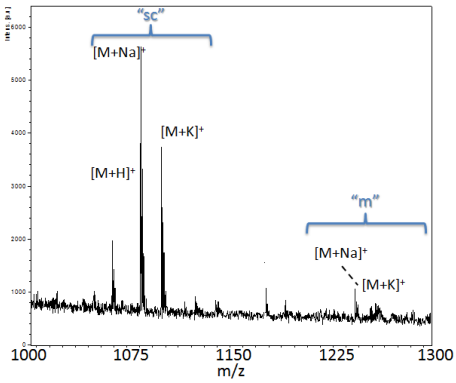

MG8_U+2 / SP4 (post-oxidation)

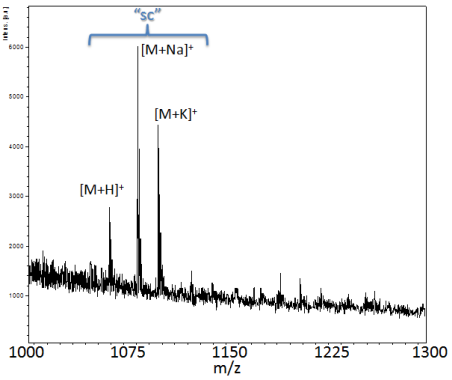

MG8_U+2 and SP4	Calc $[M+Na]^+$	Obs $[M+Na]^+$
MOrPH ("m")	1248.5	1247.6
Thiolactone ("sc")	1082.2	1081.5
Bicycle ("b")	1246.5	n/o

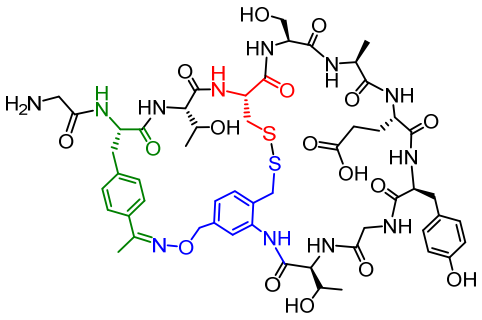

MG8_U+3 / SP4 (3h)

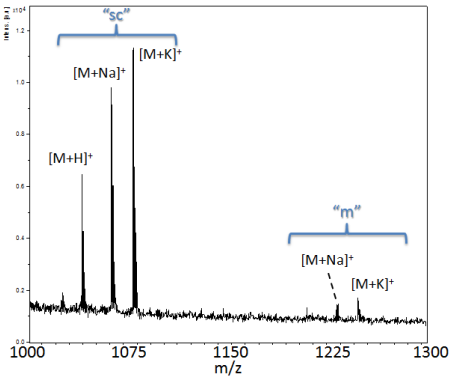

MG8_U+3 / SP4 (24h)

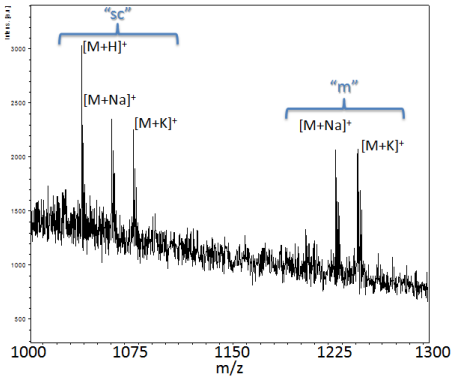

MG8_U+3 / SP4 (post-oxidation)

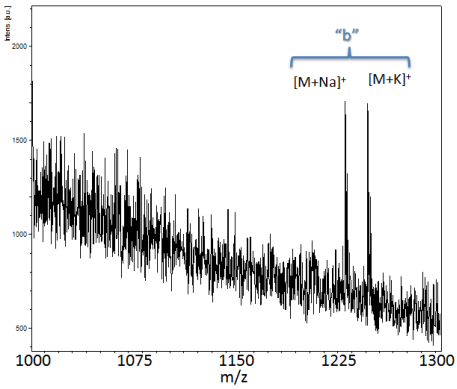

MG8_U+3 and SP4	Calc $[M+Na]^+$	Obs $[M+Na]^+$
MOrPH ("m")	1218.5	1217.8
Thiolactone ("sc")	1032.2	1051.7
Bicycle ("b")	1216.5	1215.8

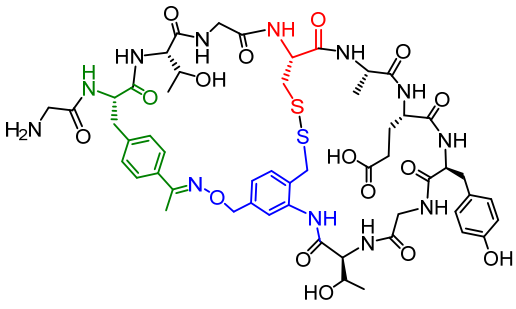

MG8_U+4 / SP4 (3h)

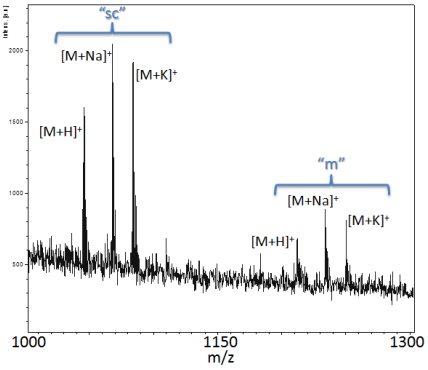

MG8_U+4 / SP4 (24h)

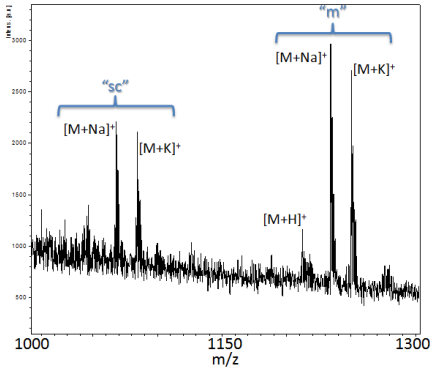

MG8_U+4 / SP4 (post-oxidation)

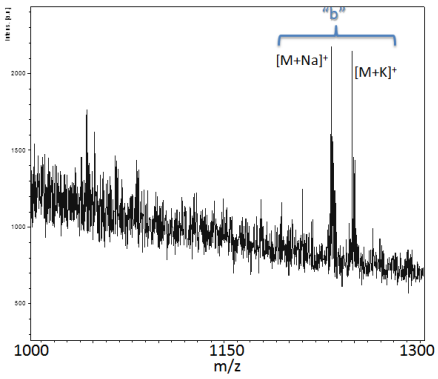

MG8_U+4 and SP4	Calc $[M+Na]^+$	Obs $[M+Na]^+$
MOrPH ("m")	1234.5	1234.3
Thiolactone ("sc")	1068.2	1068.1
Bicycle ("b")	1232.5	1232.2

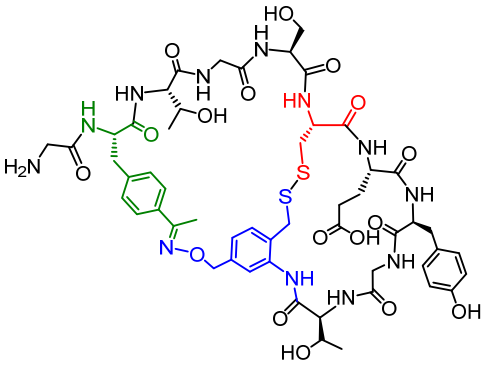

MG8_U+5 / SP4 (3h)

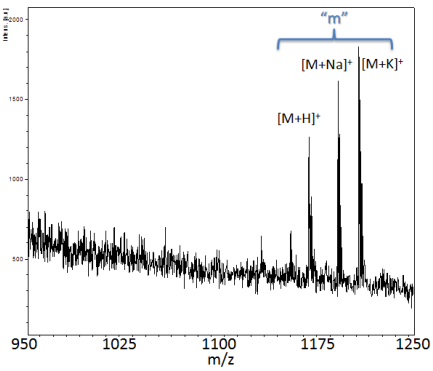

MG8_U+5 / SP4 (post-oxidation)

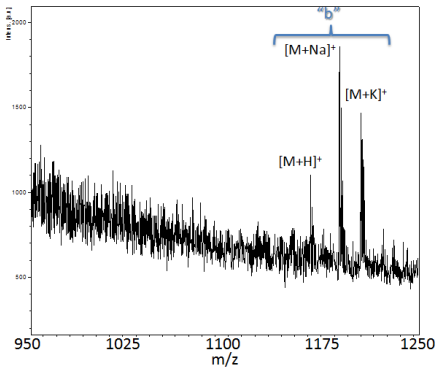

MG8_U+5 and SP4	Calc $[M+H]^+$	Obs $[M+H]^+$
MOrPH "m"	1154.4	1154.4
Thiolactone "sc"	988.1	n/o
Bicyclic MOrPH "b"	1152.4	1152.5

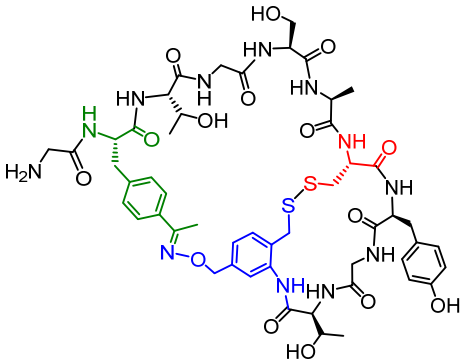

MG8_U+6 / SP4 (3h)

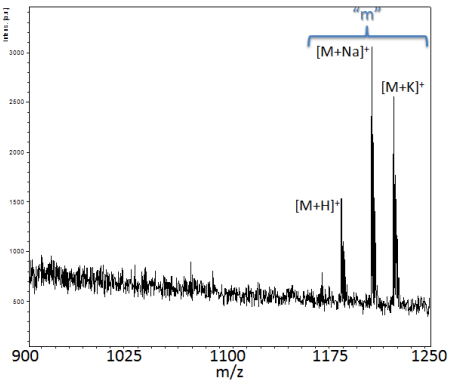

MG8_U+6 / SP4 (post-oxidation)

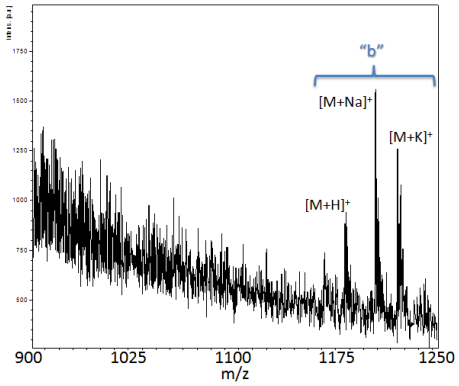

MG8_U+6 and SP4	Calc $[M+H]^+$	Obs $[M+H]^+$
MOrPH ("m")	1120.4	1120.4
Thiolactone ("sc")	954.1	n/o
Bicycle ("b")	1118.4	1118.2

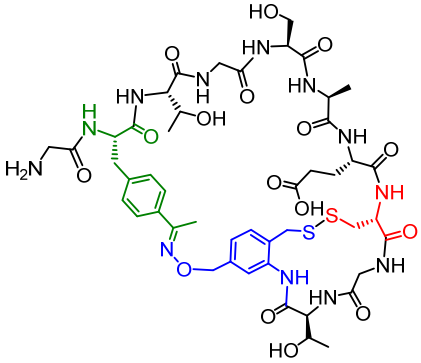

MG8_U+7 / SP4 (3h)

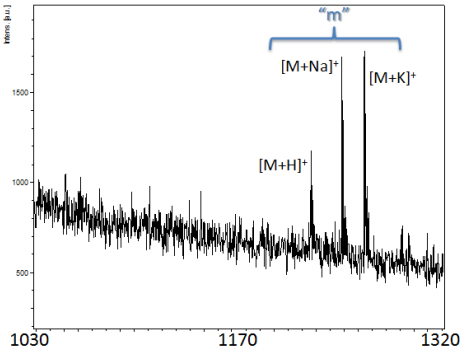

MG8_U+7 / SP4 (post-oxidation)

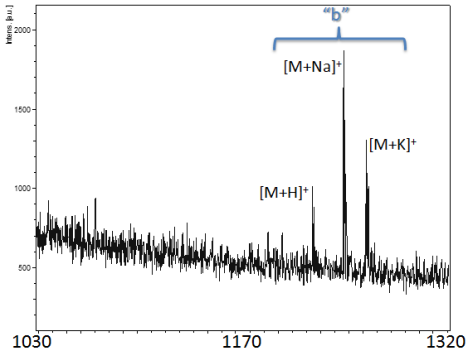

MG8_U+7 and SP4	Calc $[M+H]^+$	Obs $[M+H]^+$
MOrPH ("m")	1226.5	1226.0
Thiolactone ("sc")	1060.2	n/o
Bicycle ("b")	1224.5	1224.1

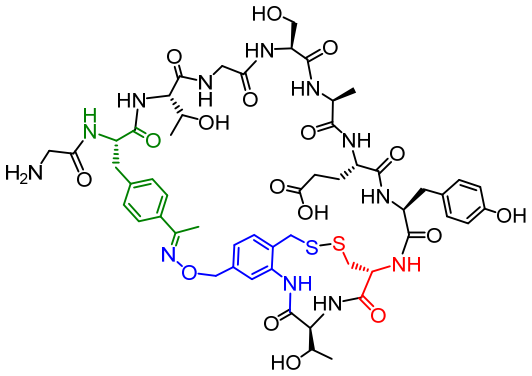

Supplementary Figure S4. MALDI-TOF MS analysis of the reactions between **2** (SP4) and the 10mer biosynthetic precursors (MG10 series, Table 1). Spectra correspond to the three hour (*left*) and 24 hour time point (*center*) after addition of **1** and one hour time point after addition of BPDS (*right*). Peaks corresponding to the proton ($[M+H]^+$), sodium ($[M+Na]^+$), and potassium ($[M+K]^+$) adducts of the MOrPH ('m'), self-cyclized thiolactone ('sc') and bicyclic product ('b') are labeled. When no self-cyclized product is formed, the 24 hr-time point spectrum is omitted as it is identical to the 3-hr spectrum. The calculated and observed *m/z* values for the proton (or sodium) adducts are provided in the table. The structure of the bicyclic product is also shown.

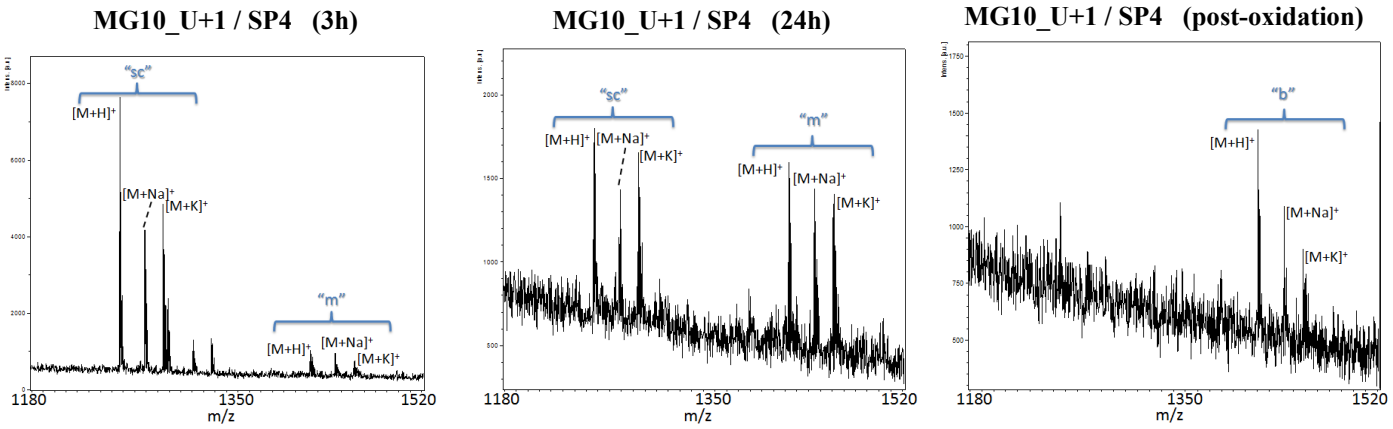

MG10_U+1 and SP4	Calc $[M+H]^+$	Obs $[M+H]^+$
MOrPH ("m")	1423.6	1422.9
Thiolactone ("sc")	1257.3	1256.8
Bicycle ("b")	1421.6	1420.9

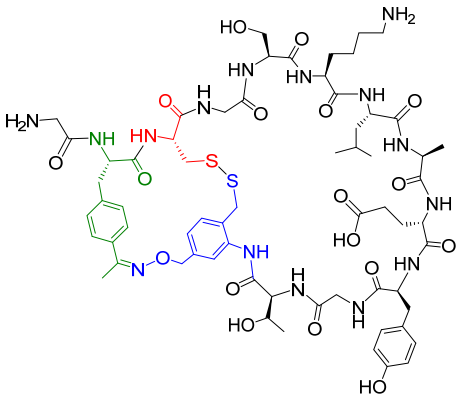

MG10_U+2 / SP4 (3h)

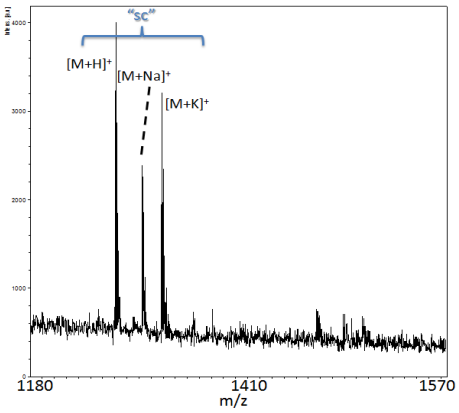

MG10_U+2 / SP4 (24h)

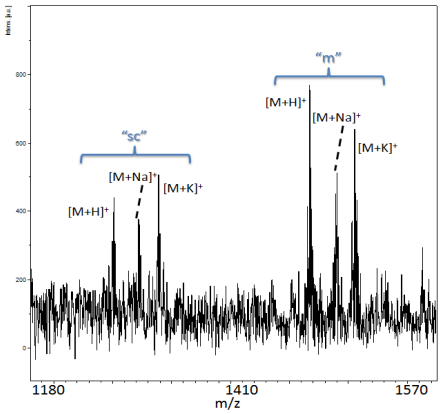

MG10_U+2 / SP4 (post-oxidation)

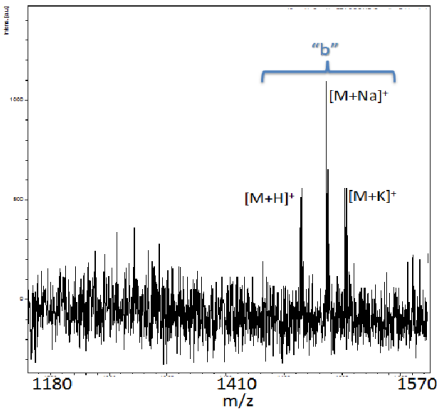

MG10_U+2 and SP4	Calc $[M+H]^+$	Obs $[M+H]^+$
MOrPH ("m")	1466.7	1467.1
Thiolactone ("sc")	1300.4	1300.9
Bicycle ("b")	1464.7	1465.0

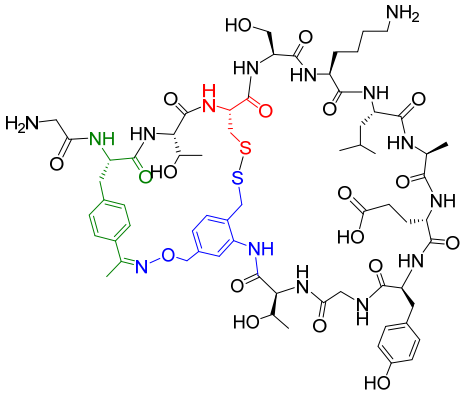

MG10_U+3 / SP4 (3h)

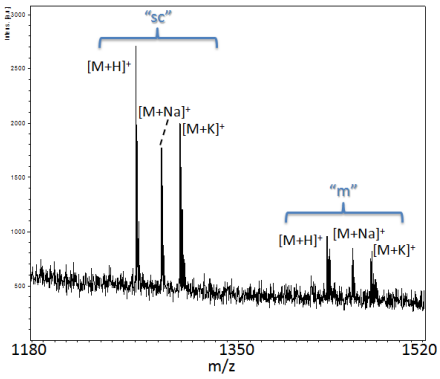

MG10_U+3 / SP4 (24h)

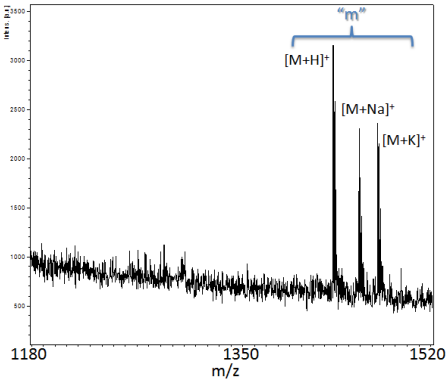

MG10_U+3 / SP4 (post-oxidation)

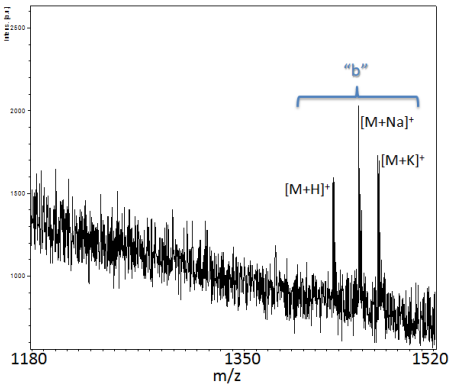

MG10_U+3 and SP4	Calc $[M+H]^+$	Obs $[M+H]^+$
MOrPH ("m")	1437.7	1437.1
Thiolactone ("sc")	1271.4	1271.0
Bicycle ("b")	1435.7	1435.0

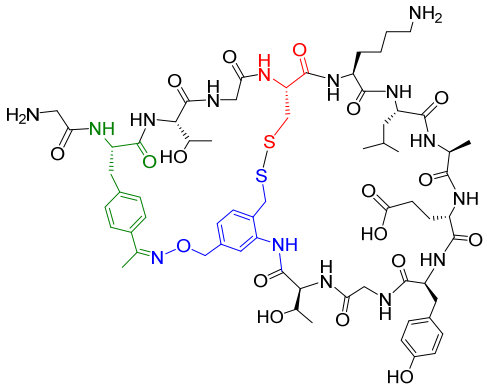

MG10_U+4 / SP4 (3h)

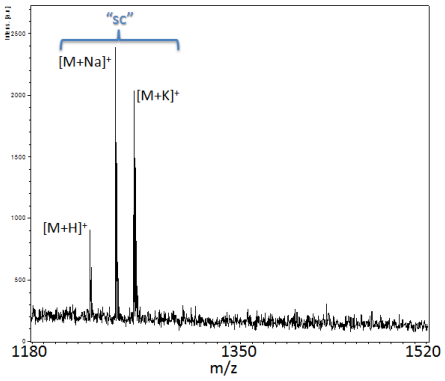

MG10_U+4 / SP4 (24h)

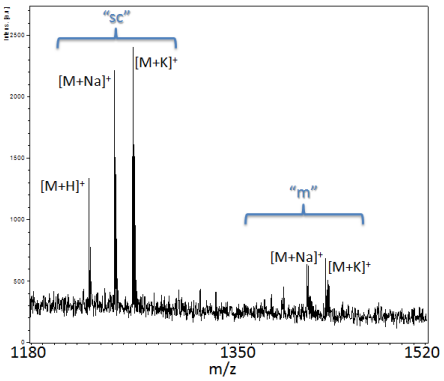

MG10_U+4 / SP4 (post-oxidation)

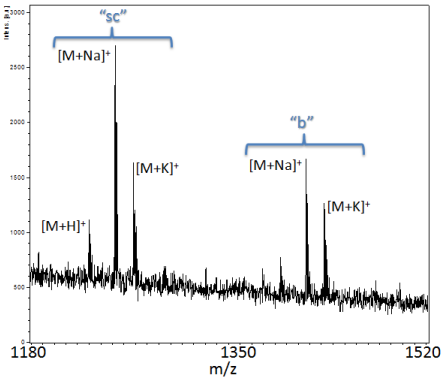

MG10_U+4 and SP4	Calc $[M+H]^+$	Obs $[M+H]^+$
MOrPH ("m")	1396.7	1396.7
Thiolactone ("sc")	1230.4	1230.6
Bicycle ("b")	1394.7	1394.9

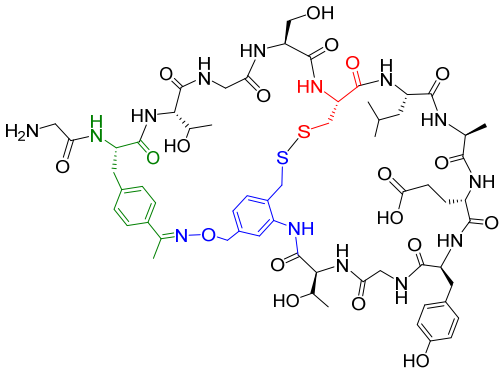

MG10_U+5 / SP4 (3h)

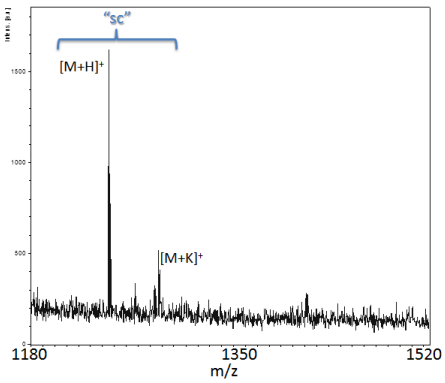

MG10_U+5 / SP4 (24h)

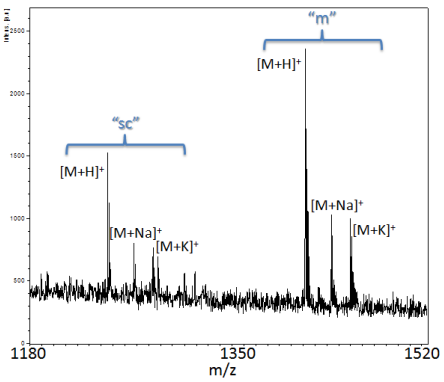

MG10_U+5 / SP4 (post-oxidation)

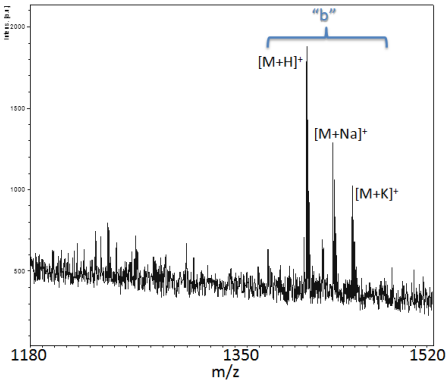

MG10_U+5 and SP4	Calc $[M+H]^+$	Obs $[M+H]^+$
MOrPH ("m")	1410.7	1411.4
Thiolactone ("sc")	1244.4	1245.2
Bicycle ("b")	1408.7	1409.3

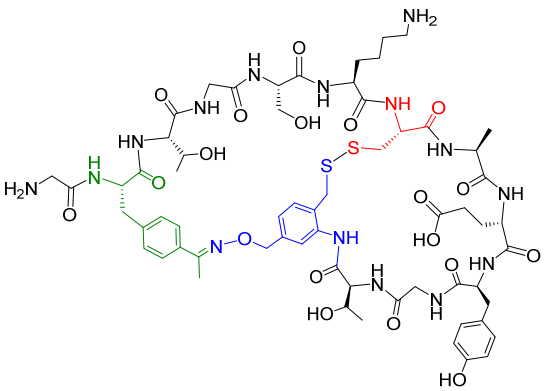

MG10_U+6 / SP4 (3h)

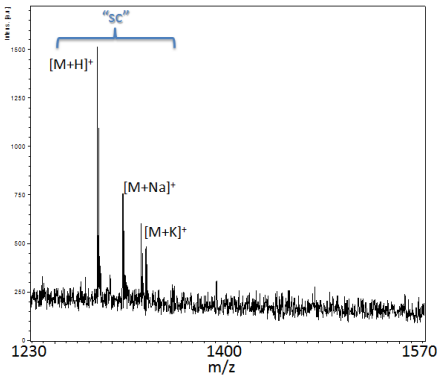

MG10_U+6 / SP4 (24h)

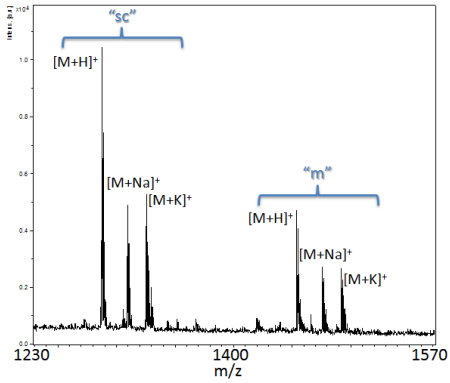

MG10_U+6 / SP4 (post-oxidation)

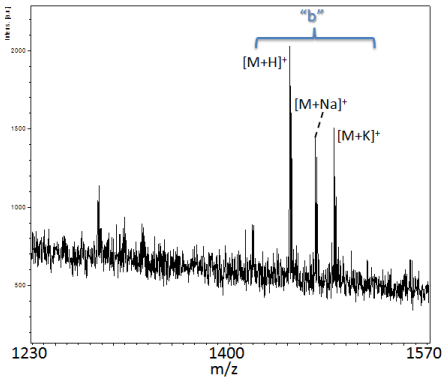

MG10_U+6 and SP4	Calc $[M+H]^+$	Obs $[M+H]^+$
MOrPH ("m")	1453.8	1453.9
Thiolactone ("sc")	1287.5	1287.7
Bicycle ("b")	1451.8	1451.9

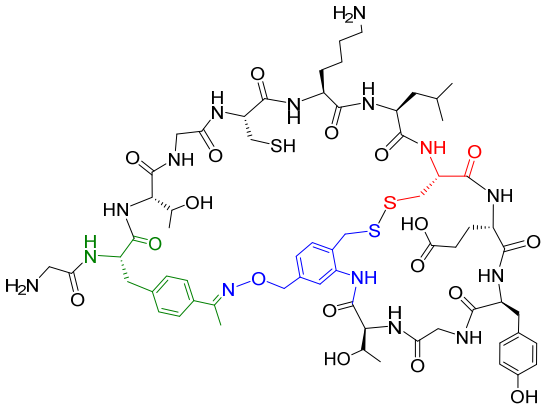

MG10_U+7 / SP4 (3h)

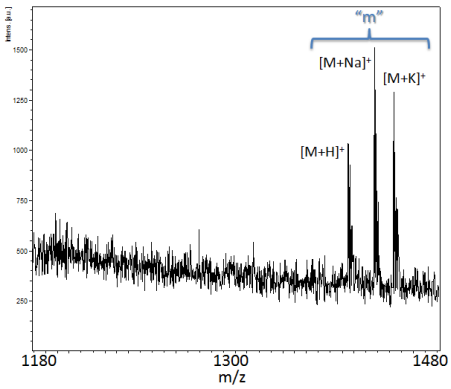

MG10_U+7 / SP4 (post-oxidation)

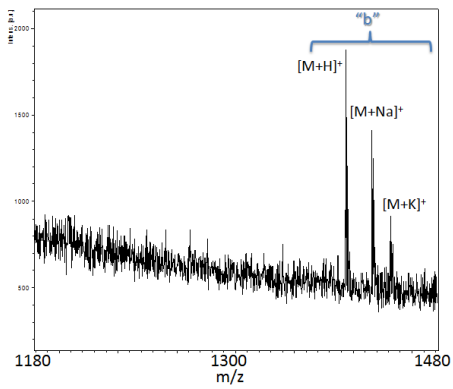

MG10_U+7 and SP4	Calc $[M+H]^+$	Obs $[M+H]^+$
MOrPH ("m")	1395.8	1395.9
Thiolactone ("sc")	1229.5	1287.7
Bicycle ("b")	1393.8	1393.9

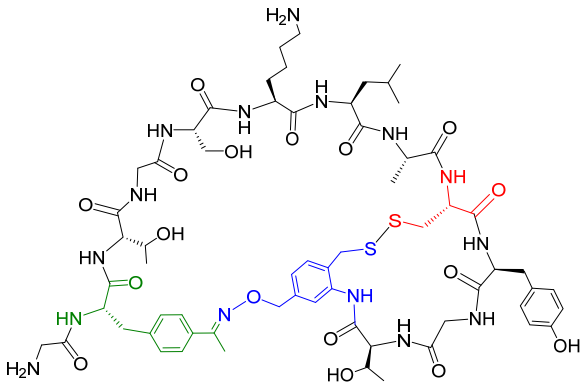

MG10_U+8 / SP4 (3h)

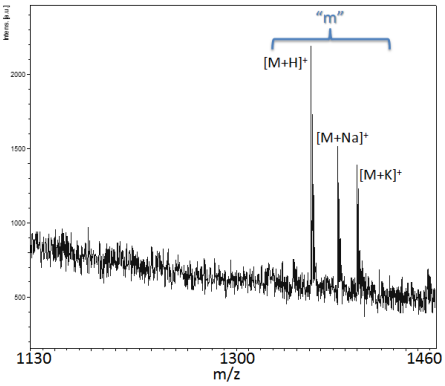

MG10_U+8 / SP4 (post-oxidation)

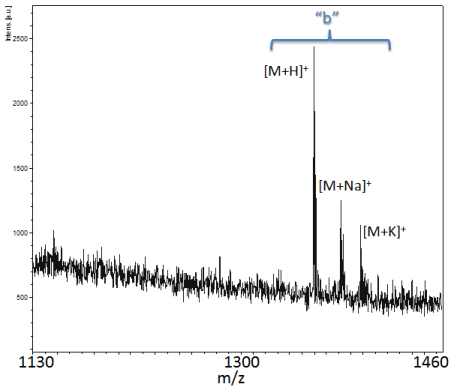

MG10_U+8 and SP4	Calc $[M+H]^+$	Obs $[M+H]^+$
MOrPH ("m")	1361.6	1361.9
Thiolactone ("sc")	1195.3	n/o
Bicycle ("b")	1359.6	1359.8

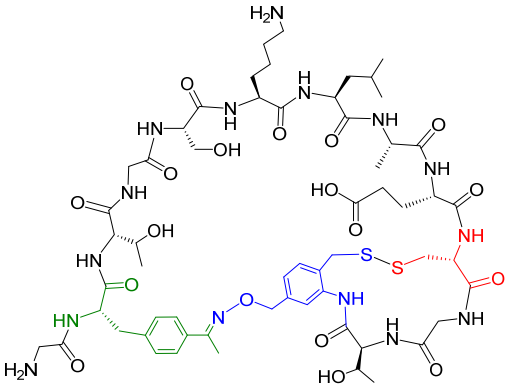

MG10_U+9 / SP4 (3h)

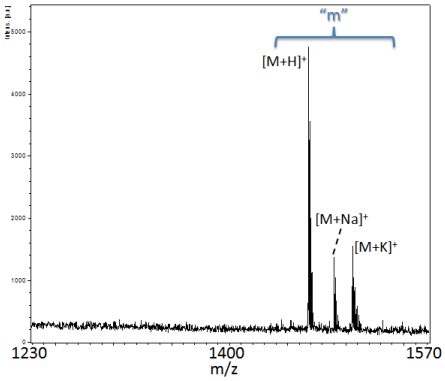

MG10_U+9 / SP4 (post-oxidation)

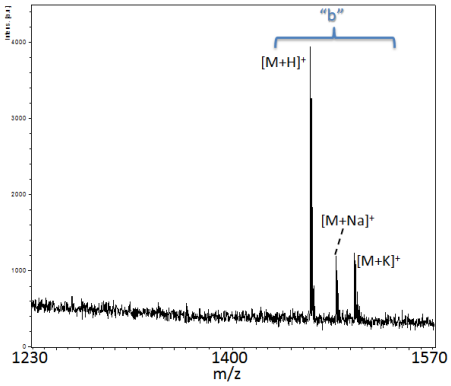

MG10_U+9 and SP4	Calc $[M+H]^+$	Obs $[M+H]^+$
MOrPH ("m")	1467.8	1467.6
Thiolactone ("sc")	1301.5	n/o
Bicycle ("b")	1465.8	1465.5

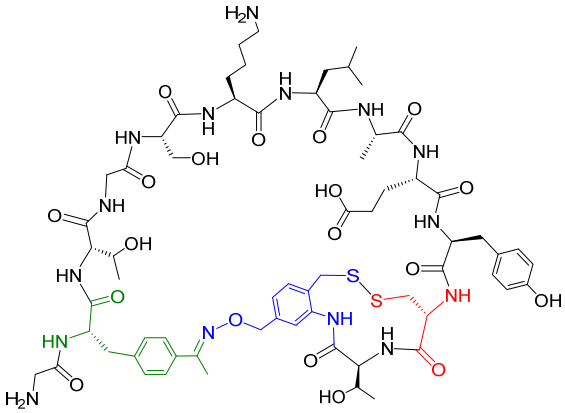

Supplementary Figure S5. Iodoacetamide thiol alkylation experiments. MALDI-TOF spectrum of post-cyclization products (6 hours) from the reaction between (A) MG8_U+4 + **1** (SP6), and (B) MG8_U+1 + **2** (SP4), after incubation with iodoacetamide (20 mM, 1 hour). Calculated and observed masses for self-cyclized and di-alkylated MOrPH products are provided.

A **MG8_U+4 / SP6 + iodoacetamide**

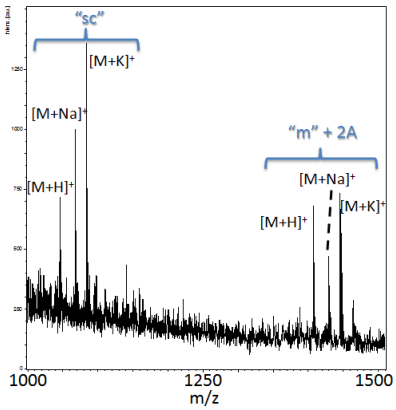

MG8_U+4 and SP6	Calc $[M+H]^+$	Obs $[M+H]^+$
MOrPH + 2A ("m" + 2 acetamide)	1407.5	1407.5
Thiolactone ("sc")	1046.2	1046.1

B

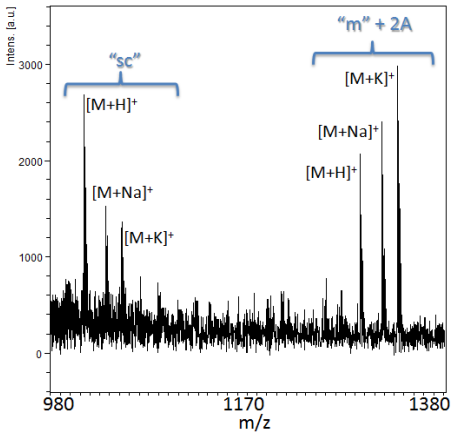

MG8_U+1 and SP4	Calc $[M+H]^+$	Obs $[M+H]^+$
MOrPH + 2A ("m" + 2 acetamide)	1296.4	1295.8
Thiolactone ("sc")	1016.1	1015.5